Title
Investigating the effects of ADP-ribosylation factor 4 (ARF4) on pattern separation and dendritic spine development

Author
Yim, Sachi Jain

Publication Date
2012

Peer reviewed|Thesis/dissertation

INVESTIGATING THE EFFECTS OF ADP-RIBOSYLATION FACTOR 4 (ARF4) ON PATTERN SEPARATION AND DENDRITIC SPINE DEVELOPMENT

by

Sachi Jain Yim

DISSERTATION

Submitted in partial satisfaction of the requirements for the degree of

DOCTOR OF PHILOSOPHY

in

Biomedical Sciences

in the

GRADUATE DIVISION

of the

UNIVERSITY OF CALIFORNIA, SAN FRANCISCO

I dedicate this dissertation to my parents, Jagdish and Sanae Jain, and to my husband, Jeffrey Yim.

ACKNOWLEDGMENTS

I would like to sincerely thank my thesis committee members – Dr. Eric Huang, Dr. Steven Finkbeiner, and Dr. Yadong Huang – for their excellent advice and guidance throughout my graduate career. I am very grateful to them for the time and effort they spent critiquing my manuscript and listening to my thesis committee meeting presentations. In particular, I would like to thank my advisor, Dr. Yadong Huang, for his consistent support and encouragement for the past five years. Dr. Huang has been instrumental in helping me develop my critical thinking skills, and he has been a valuable source of advice when I needed to troubleshoot experiments or discuss project ideas. Dr. Huang also taught me several important life lessons, including the following: think carefully before throwing anything away, because you never know when you might need it; always expect more from yourself than you think you should; and do not stop in the middle of an experiment, even if you think it might not work.

I would also like to express my gratitude toward all of the Huang lab members, who have taught me much of what I know about lab techniques and the field of neurodegenerative disease. In particular, I would like to thank Seo Yeon Yoon, Lei Zhu, Jens Brodbeck, Jessica Dai, and David Walker for their technical help and discussions about my manuscript, and for being my co-authors. I am grateful for several of the friendships I developed in the lab, and I especially thank Laura Leung and Seo Yeon Yoon for enjoyable lunchtime chats, as well as for their empathy when I encountered difficult experimental situations. Jessica Dai, a talented undergraduate summer intern, was a joy to mentor and reminded me of the importance of scientific curiosity. The entire

Gladstone community has been fantastic, and the level of talent and scientific rigor I observed at the Gladstone is unlike anything I have seen before.

I could not have completed the graduate school journey without the love and support of my parents, and there are not enough pages to write about how much they have encouraged me from my childhood onward. From my father, I learned the importance of discipline and being a lifelong learner. He has never ceased to amaze me with his broad knowledge of history and world events, and I have many joyful childhood memories of taking walks with him as he passed on his wisdom to me. My mother taught me the value of "striking while the iron is hot," or seizing opportunities the moment they present themselves. Her creativity and loyalty have left a deep impression on me, and I continue to seek her advice to this day.

During one of my most challenging times in graduate school, I was extremely fortunate to meet my now husband, Jeffrey Yim. He has been amazingly patient towards and supportive of me, and he has been a very calming influence in my life. He is one of the most generous and thoughtful people I have ever met, and he has always encouraged me to express my ideas and opinions. I deeply admire him for his willingness to put other people's needs above his own, and I look forward to a lifetime of learning with him.

I am truly thankful for the many family members, friends and colleagues who have helped me reach the culmination of my Ph.D. research. As this chapter of my life comes to an end, I am eagerly anticipating what the future will bring.

CONTRIBUTIONS

Seo Yeon Yoon genotyped and perfused the mice used for this study. Lei Zhu collaborated by conducting the electrophysiology experiments. Jens Brodbeck contributed to the project through the initial development of the dendritic spine quantification protocol. Jessica Dai was an undergraduate student intern who assisted with data collection and analysis. David Walker collaborated by developing a PCR protocol to determine the Arf4 gene trap insertion site. Yadong Huang was the principal investigator who supervised the project and assisted with the editing of the manuscript.

ABSTRACT

Investigating the Effects of ADP-Ribosylation Factor (ARF) 4 on Pattern Separation and Dendritic Spine Development in Mice

Sachi Jain Yim

The ability to distinguish between similar experiences is a critical feature of episodic memory and is primarily regulated by the dentate gyrus (DG) region of the hippocampus. However, the molecular mechanisms underlying such pattern separation tasks are poorly understood. We report a novel role for the small GTPase ADP ribosylation factor 4 (Arf4) in controlling pattern separation by regulating dendritic spine development. $Arf4^{+/-}$ mice at 4–5 months of age display severe impairments in a pattern separation task, as well as significant dendritic spine loss and smaller miniature excitatory post-synaptic currents (mEPSCs) in granule cells of the DG. Arf4 knockdown also decreases spine density in primary neurons, whereas Arf4 overexpression promotes spine development. A constitutively active form of Arf4, Arf4-Q71L, promotes spine density to an even greater extent than wildtype Arf4, whereas the inactive Arf4-T31N mutant does not increase spine density relative to controls. Arf4's effects on spine development are regulated by ASAP1, a GTPase-activating protein that modulates Arf4 GTPase activity. ASAP1 overexpression decreases spine density, and this effect is partially rescued by concomitant overexpression of wildtype Arf4 or Arf4-Q71L. In addition, Arf4 overexpression rescues spine loss in primary neurons from an Alzheimer's disease-

related apolipoprotein (apo) E4 mouse model. Our findings reveal that Arf4 is a critical modulator of pattern separation and regulates dendritic spine development both *in vitro* and *in vivo*.

TABLE OF CONTENTS

LIST OF FIGURES

CHAPTER 1

Introduction/Literature Review

Dendritic Spines: The Loci of Synapses

The extensive connections that neurons form with each other via axons and dendrites serve as the cellular basis for higher-order cognitive functions in the mammalian brain (Segal, 2005; Hotulainen and Hoogenraad, 2010). These intricate networks of neuronal communication occur via synapses, which are specialized junctions that transmit information from presynaptic axon terminals to regions on the postsynaptic dendrite. Synapses are widely regarded as memory storage sites in the brain, and the precise control of synaptic development and connectivity is crucial for proper network formation (Calabrese et al., 2006; Lippman and Dunaevsky, 2005).

Most synapses in the mature brain occur on bulbous, actin-rich protrusions along the main dendrite shaft that are known as dendritic spines. Dendritic spines were first observed over a century ago by Ramon y Cajal, who described how the dendrites of chicken Purkinje cells appeared to be "bristling with points or short spines" (Cajal, 1888). Since then, the molecular underpinnings of spine development and ultrastructure have been extensively investigated using electron microscopy, immunostaining and, more recently, live two-photon imaging (Yuste and Bonhoeffer, 2004). Spines serve a variety of purposes, including the compartmentalization of local signaling pathways and the modification of synaptic potentials (Yuste 2011; Hotulainen and Hoogenraad, 2010). Spines emerge soon after dendritic processes are extended from neurons during early

development, and they can be formed either from filopodial precursors or through the conversion of an existing shaft synapse (Bhatt et al., 2009; Segal, 2005). Spines generally develop concurrently with the growth of presynaptic elements, indicating that extrinsic cellular cues likely influence spine formation (Lippman and Dunaevsky, 2005).

Throughout development and adulthood, spines are highly motile and undergo changes in number and morphology that accompany neuronal circuit remodeling (Penzes et al., 2011). Mature spines generally consist of a head region, which contains the postsynaptic density (PSD), and a neck that connects the spine to the dendrite shaft. Dendritic protrusions are generally classified into one of the following four categories based on the neck length and the presence or absence of a head: stubby spines, which lack a well-defined neck; mushroom spines with a large, bulbous head and short neck; thin spines with a longer neck and small head; and filopodia, which are long headless extensions (Vanderklish and Edelman, 2002). Spine morphology correlates with synaptic strength and structural plasticity; for instance, thin ("learning") spines are highly motile and likely to respond to activity-induced changes, whereas mushroom ("memory") spines have larger post-synaptic densities (PSDs) and are more stable (Peebles et al., 2010; Bourne and Harris, 2007). Reductions in both thin (Dumitrui et al., 2010) and mushroom (Perez-Cruz et al., 2011) spine densities have been associated with learning and memory deficits, indicating that the correct balance of these spine subtypes is critical for healthy cognitive function.

Aberrations in spine density and morphology are associated with a number of neurological disorders, including Alzheimer's disease (AD) (Penzes and Vanleeuwen, 2011; Fiala et al., 2002; Tackenberg et al., 2009). AD is characterized by the progressive

loss of cognitive function, and the loss of spines and synapses is the best correlate of these learning and memory impairments (Knobloch and Mansuy, 2008; Terry et al., 1991). ApoE4 is the major genetic risk factor for AD (Strittmatter et al., 1993; Roses 1996), and it is associated with learning and memory impairments both in humans (Caselli, 2009) and in mice (Raber et al., 1998; Andrews-Zwilling et al., 2010). ApoE4 transgenic mice show reduced dendritic spine density in the hippocampus and cortex compared to their apoE3 controls (Ji et al., 2003; Dumanis et al., 2009), and apoE4 dose correlates inversely with spine density in both normal and AD patient brains (Ji et al., 2003). These findings indicate a strong association between the pathogenic apoE4 isoform and impairments in spine development and/or maintenance.

Role of the Actin Cytoskeleton and Small GTPases in Dendritic Spine Biology

The dysregulation of spine development in neurodegenerative disorders such as AD and frontotemporal dementia (FTD) stems largely from degradation of the actin cytoskeleton (Penzes and Vanleeuwen, 2011; Gong and Lippa 2010). As the major cytoskeletal component of dendritic spines, actin plays a pivotal role in spine development and morphology (Hotulainen and Hoogenraad, 2010; Sekino et al., 2007). Both the monomeric (G-actin) and filamentous polymeric (F-actin) forms of actin are present in spines, and the ratio between these two forms influences dendritic spine development, morphology, and dynamics (Cingolani and Goda, 2008). The extensive network of straight and branched actin filaments underneath the PSD modulates spine head structure and stabilizes postsynaptic proteins. The PSD contains numerous actin-binding and actin

cross-linking proteins, and down-regulation of these proteins impairs spine development and maturation (Hering and Sheng, 2003; Ivanov et al., 2009).

Among the regulators of actin cytokeleton rearrangement and spine development are members of the Ras superfamily of small GTPases. Small GTPases, also known as guanine nucleotide binding proteins or G proteins, are biochemically similar to heterotrimeric G α subunits and share a set of conserved G box GDP/GTP-binding motif elements (Wennerberg et al., 2005). Small GTPases function as molecular switches by alternating between an inactive GDP- and an active GTP-bound state to regulate downstream cellular processes. This cycle is regulated by guanine nucleotide exchange factors (GEFs), which promote GDP displacement in favor of GTP, and GTPase activating proteins (GAPs), which facilitate the hydrolysis of GTP to GDP (Donaldson and Jackson, 2011).

The Ras small GTPase superfamily consists of five subfamilies – Ras, Rho, Rab, Ran, and Arf – with diverse roles in actin reorganization, intracellular vesicular transport, protein trafficking, and cell cycle progression (Wennerberg et al., 2005; Csepanyi-Komi et al., 2012). Of these small GTPases, Rho, Ras, and Arf proteins have reported roles in dendritic spine development and maintenance. Within the Rho branch of GTPases, Rac1 overexpression increases spine density, whereas RhoA inhibits spine development (Tashiro et al., 2000; Nakayama et al., 2000). The activated Ras/MAP kinase pathway is required for filopodia formation *in vitro* (Wu et al., 2001), and mice overexpressing Ras specifically in their neurons show increased spine density in the neocortex (Gartner et al., 2005). In the Arf family, constitutively active Arf6 promotes spine formation (Choi et al., 2006), and several regulators of the Arf6 GTP/GDP cycle interact with the postysynaptic

protein PSD-95 to influence synapse development (Choi et al., 2006; Sakagami et al., 2008).

Structure and Function of ADP Ribosylation Factors

ADP ribosylation factor (Arf) GTPases are important regulators of vesicular transport and actin cytoskeletal assembly in both neuronal and non-neuronal cells. Although several reports have described the effects of Arf6 on dendritic spine development and dendrite arborization (Jaworski , 2007; Choi et al., 2006), little is known about the potential neurobiological roles of other Arf family members.

The mammalian Arf family is comprised of six proteins, Arf1–6, which are grouped into three classes based on sequence homology. Class I consists of Arf1–3, Class II consists of Arf4–5, and Arf6 is the sole member of Class III (Donaldson and Jackson, 2011; D'Souza-Schorey and Chavrier, 2006). Class I and Class II Arfs are mainly localized to the Golgi apparatus, whereas Arf6 is concentrated in the plasma membrane and some endosomal compartments (Myers and Casanova, 2008). Arfs contain four consensus sequences involved in guanine nucleotide binding and hydrolysis, as well as two switch regions flanking a mobile interswitch region. The switch I and switch II regions mediate the interaction of Arfs with their GEFs and GAPs. Upon GTP binding, the interswitch region displaces the N-terminal amphipathic helix, allowing for membrane insertion and subsequent Arf-GTP activity (Gillingham and Munro, 2007).

The Arf GTPase cycle is highly regulated by Arf GEFs and GAPs. Arf GEFs share a central catalytic Sec7 domain and can be divided into several classes based on overall structure and domain organization: GBF/BIG, ARNO/cytohesin, EFA6, BRAG,

and FBX8. Of these, GBF/BIG proteins localize mainly to the Golgi and are sensitive to the fungal toxin brefeldin A (BFA) (Casanova, 2007). The two major groups of Arf GAPs are the Arf GAP1 type, which includes ArfGAP1 and Git1/2, and the AZAP type, consisting of ASAP, AGAP, ARAP, and ACAP (Randazzo and Hirsch, 2004).

Arfs exert their biological effects through an extensive network of effectors that include vesicle coat proteins, phospholipid-metabolizing enzymes, and actin regulatory molecules (Nie et al., 2003). All Arfs activate phospholipase D (PLD) and PIP kinases, leading to the conversion of PIP to PIP2. PIP2 binds and activates actin regulatory proteins, thereby influencing actin cytoskeleton assembly (Myers and Casanova, 2008). Class I Arfs recruit coat protein complex I (COP1), adaptor-protein complex, and GGA proteins during various steps of the early secretory pathway. The Class III Arf, Arf6, regulates clathrin recruitment at the plasma membrane, and it is also implicated in clathrin-independent ligand internalization (D'Souza-Schorey and Chavrier, 2006).

Arf4: Diverse Cellular Functions and Emerging Roles in Neurobiology

Compared to the extensive literature detailing the functions of Class I and Class III Arfs, relatively few studies have examined the roles of Class II Arfs. Arf4 is a 20kDa, 180-amino acid Class II Arf that consists of six exons and five introns, with protein translation beginning in exon 1 (Lebeda and Haun, 1999). Arf4 is involved in diverse cellular processes including breast cancer cell migration (Jang et al., 2012), rhodopsin trafficking (Mazelova et al., 2009), and suppression of Bax-induced cell death (Woo et al., 2009). Like other Arf family members, Arf4 cycles between a GTP- and GDP-bound state, and this cycling activity is regulated by GAPs and GEFs. Two mutant forms of Arf4 – Arf4-

T31N and Arf4-Q71L – remain constitutively bound to GDP or GTP, respectively, and have different physiological effects according to their activity status (Kim et al., 2003). Although an Arf4-specific GEF has not yet been identified, the Arf GAP ASAP1 has been shown to bind to and have GTPase activity toward Arf4 *in vitro* (Mazelova et al., 2009).

Investigations into the potential neurobiological roles of Arf4 are still in a nascent stage. Previous studies have detected filament fragmenting in the rod photoreceptors of transgenic *Xenopus laevis* expressing a mutant form of Arf4 (Mazelova et al., 2009). These findings indicate that Arf4 functions critically in actin cytoskeletal assembly and might be involved in dendritic spine development. Furthermore, Arf4 mRNA is highly expressed in the rat hippocampus at postnatal day 7, and its expression remains particularly strong in the DG through postnatal day 21 (Suzuki et al., 2001). Arf4's expression pattern in the brain suggests that it could play a role in hippocampal learning and memory processes, particularly those specifically associated with the DG.

Pattern Separation and the Dentate Gyrus

In the adult mammalian brain, the hippocampus plays a central role in the encoding, storage, and retrieval of spatial and episodic memory. Impairments in these processes are associated with progressive neurodegenerative disorders such as AD (Yassa and Stark, 2011; Burgess et al., 2002). A critical component of episodic memory is a phenomenon known as pattern separation, or the ability to form distinct representations of similar inputs (Schmidt et al., 2011; Aimone et al., 2011; Treves et al., 2008; Yassa and Stark, 2011). The process of distinguishing between similar memory representations is vital for

enhancing memory accuracy. Without pattern separation, the acquisition of new memories would replace similar previously stored information, and subtle distinctions between episodes would be lost (McClelland et al., 1995; Norman and O'Reilly, 2003). Studies indicate that pattern separation becomes less effective during normal aging (Toner et al., 2009) and in mild cognitive impairment (MCI), a disorder that likely represents an early stage of AD (Yassa et al., 2010)

Several lines of evidence have established the dentate gyrus (DG) subregion of the hippocampus as a critical mediator of pattern separation. The idea that the DG might function as a pattern separator first arose from early hippocampal modeling work, which suggested that the recurrent collaterals within the CA3 hippocampal subregion are ideally suited to store episodic memory (Marr, 1971). Subsequent studies indicated a need for a pattern separation device upstream of the CA3 to form discrete memory representations from correlated patterns (Kropff and Treves, 2007). Anatomically, the DG is well-situated in the trisynaptic hippocampal circuit to de-correlate incoming network patterns from the entorhinal cortex (EC) (Schmidt et al., 2011; Aimone et al., 2011). At the cellular level, DG granule cells facilitate pattern separation through their sparse pattern of activity and powerful "detonator" synapses. Only 2– 4% of DG granule cells show activity in a particular environment compared to 30–40% of CA1 pyramidal neurons (O'Keefe and Dostrovsky, 1971; Jung and McNaughton, 1993), and a single mossy fiber is powerful enough to fire a downstream CA3 neuron (Henze et al., 2002). Furthermore, behavioral studies have shown that animals with impaired DG function are unable to differentiate between similar events or objects. For example, lesions of the rodent DG disrupted spatial pattern separation for both reference and working memory (Gilbert et

al., 2001; Morris et al., 2012), and mice lacking NMDA receptors specifically in DG granule cells were impaired in a contextual fear conditioning pattern separation task (McHugh et al., 2007). These findings point to a clear role for the DG in de-correlating similar input patterns.

Summary and Objectives

Dendritic spines are important loci for synaptic plasticity, and their development and maintenance are regulated by multiple factors that include small GTPases. The loss of spines is the best correlate for learning and memory deficits observed in AD. Patients with mild cognitive impairment, a syndrome associated with increased AD risk, show difficulties in performing certain memory tasks such as pattern separation. Anatomical and behavioral studies point to the DG region of the hippocampus as the central mediator of pattern separation. However, the potential relationship between DG-dependent pattern separation tasks and granule cell dendritic spine development and activity is poorly understood.

The objective of this study was to examine the roles of the small GTPase Arf4, which is highly expressed in the DG and is involved in actin regulation, in pattern separation and dendritic spine development. For our *in vivo* studies, an $Arf4^{+/-}$ mouse line was generated using a gene-trapping technique. $Arf4^{+/-}$ and WT mice underwent pattern separation and Morris water maze behavioral tests to assess cognitive performance. Rotarod, elevated plus maze, and open field tests were used to examine non-hippocampal behavior. Brains from WT and $Arf4^{+/-}$ mice were Golgi-stained for quantification of spine

density and morphology in the DG and CA1 hippocampal regions, and the amplitude and frequency of mEPSCs were recorded from DG granule cells.

To determine whether Arf4 influences spine development *in vitro*, primary neurons were transfected with GFP-β-actin alone or together with HA-tagged Arf4-wildtype (WT), Arf4-T31N, or Arf4-Q71L, followed by quantification of spine density and morphology. A GFP-tagged Arf4 shRNA construct was used to study the effects of knocking down Arf4 on spine development. ASAP1, an Arf GAP with GTPase activity toward Arf4, was transfected with Arf4-WT or Arf4-Q71L to investigate its role in Arf4-regulated spine development. Arf4's potential use as a therapeutic agent for dendritic spine loss was investigated by overexpressing Arf4 in NSE-apoE4 primary neurons, followed by spine density and morphology analysis.

CHAPTER 2

Materials and Methods

Generation of Arf4$^{+/-}$ mice. The Arf4$^{+/-}$ mouse model was established based on an embryonic stem cell line from BayGenomics (CSH658). The ES cell line contains a gene trapping construct (pGT1lxf) in intron 1 of the Arf4 gene, located upstream of the gene encoding the β-galactosidase/neomycin-resistance fusion protein. The FastStart Taq DNA Polymerase dNTPack kit (Roche) was used to generate candidate forward primers designed for 200–500 base pair intervals of intron 1 of the Arf4 gene. One common reverse primer in the β-galactosidase reporter, RT416, was applied in all reactions (5'-GTCCTCTGGTGCTCAAAGACC-3'). Amplification with forward primer P8 (5'-TGGAAGCACAGGCCTTTAATCC-3'), located in intron 1, yielded a distinct PCR product of approximately 800kb. PCR conditions were 34 cycles at 95°C for 30s, 57°C for 30s, and 72°C for 1 min, followed by a final extension at 72°C for 7 min. The PCR product was verified by sequencing.

The CSH658 ES cells were microinjected into C57Bl6 blastocysts to yield chimeras, which were identified by coat color. A chimeric male was crossed with wildtype C57Bl6 females, and germline transmission resulted in heterozygote males and females of the F1 generation. Mice were backcrossed to the C57Bl6 background for at least 5 generations for all studies, producing both Arf4$^{+/-}$ and WT mice. C57Bl6 mice were purchased from the Jackson Laboratories. All animal procedures were approved by the Gladstone Institutes and the University of California San Francisco Animal Care and Use

Committees.

Genotyping of Arf4$^{+/-}$ mice. Genotype of Arf4$^{+/-}$ mice was determined by using 2 parallel PCRs. The first pair of primers consisted of the forward primer I8.1 (5'-AGCATATTCCCCTACTTAACTGTGTCTC-3') and the reverse primer I8.1 Rev (5'-CAAAGGTGTTGCGGCACAGA-3'), both of which are in intron 1. The second pair of primers consisted of P8 and RT416, the same pair used to characterize the ES cell line. PCR conditions were as described for identification of the gene trap insertion site. DNA was prepared from 0.5cm of cut tail from 21-day-old mice and digested overnight with sodium chloride-tris-EDTA buffer, followed by deactivation with Proteinase K. PCR products were electrophoresed on 2% agarose gels and stained with ethidium bromide.

Preparation of mouse brain tissues and Neuro-2A cell lysates. Brains from WT or Arf4$^{+/-}$ mice were collected after a 1 min transcardial perfusion with saline. The hippocampus and cortex were dissected from one hemibrain of each mouse and were homogenized with low detergent lysis buffer as previously described (Harris et al., 2003). Samples were centrifuged at 35,000 rpm for 30 min at 4ºC using a TLA 100.2 rotor of an Optima TL Ultracentrifuge (Beckman Coulter, Brea, CA) and the lysates were analyzed for Arf4 using western blot. Neuro-2A cells were lysed with low detergent buffer and centrifuged at 12,000 rpm for 10 min at 4ºC, and supernatant was collected for western blot analysis. Rabbit anti-Arf4 was from Protein Tech Group (Chicago, IL), and rabbit anti-actin was from Sigma. Horseradish peroxidase-coupled anti-goat IgG was from Dako (Carpentaria, CA).

Primary neuron preparation, transfection, and immunocytochemistry. Mixed hippocampal and cortical neuron cultures were prepared from E18-19 mice and grown on poly-L-lysine-coated coverslips as reported (Brodbeck et al., 2008). Neurons were fixed in PBS containing 4% paraformaldehyde, permeabilized with 0.1% Triton X-100, and blocked with 5% normal goat serum in PBS for 1 hour at room temperature. Neurons were incubated for one hour at room temperature with primary antibodies to goat HA (1:500, Novus Biologicals, Littleton, CO) or rabbit Flag (1:500, Sigma). Secondary fluorophore-conjugated antibodies included donkey anti-goat Alexa594, donkey anti-goat Alexa647, and donkey anti-rabbit Alexa594 (1:1000, Invitrogen).

Image analysis and quantification. For fluorescent cells, serial confocal images were taken with a BX60 BioRad Radiance 40X dry objective with a digital zoom factor of 2 for low magnification or of 4 for high magnification images. Z-stack sections were merged using LaserSharp2000 software. Neurons were selected randomly and 1 to 2 equivalent-length dendritic segments from each neuron were chosen for quantification of protrusions. Protrusion density and morphology were manually quantified using ImageJ software, according to criteria described (Vanderklish and Edelman, 2002).

cDNA and small hairpin RNA constructs. HA-tagged human wildtype Arf4 was a gift from JD Lee (Scripps Research Institute, La Jolla, CA) (Kim et al., 2003). Arf4-HA point mutants (Arf4-HA-T31N and Arf4-HA-Q71L) were generated using the QuikChange II XL Site-Directed Mutagenesis kit (Strategene). mCherry-tagged human Arf4 was a gift from Paul Melancon (University of Alberta, Edmonton, Canada) (Chun et al., 2008). The

FUGW2-GFP and GFP-β-actin plasmids were gifts from Lennart Mucke and Steve Finkbeiner, respectively (Gladstone Institutes, San Francisco, CA) (Peebles et al., 2010, Chen et al., 2005). Arf4-shRNA1 and Arf4-shRNA2 constructs were expressed under the U6 promoter using the FUGW2 vector. The target sequences used for the Arf4 shRNAs are as follows: 5'-TCTGGTAGATGAATTGAGA-3' (Arf4-shRNA1) and 5'-AGATAGCAACGATCGTGAA-3' (Arf4-shRNA2). Flag-tagged murine ASAP1 cDNA, a gift from Paul Randazzo (National Cancer Institute, Bethesda, MD), was expressed in the pCR2.1 vector (Brown et al., 1998).

Staining of mouse brains. For β-galactosidase staining, brains from 4.5-month-old $Arf4^{+/-}$ mice were removed, frozen in OCT compound, and sectioned at a thickness of 10μm using a Leica CM1900 cryostat. Sections were washed 3 times in 0.02% Nonidet P-40/PBS, fixed in 4% paraformaldehyde in PBS for 10 min at room temperature, and stained in PBS with 5mM $K_3Fe(CN)_6$, 5mM $K_4Fe(CN)_6$, 2mM $MgCl_2$, 0.01% sodium deoxycholate, 0.02% Nonidet-P-40, and 1 mg/ml X-gal at 37°C for 16h. After a series of ethanol washes, sections were cleared in xylene and mounted with Cytoseal.

For Golgi staining, 4.5-month-old $Arf4^{+/-}$ and WT littermates were stained in parallel using modified Golgi-Cox impregnation of neurons following the manufacturer's protocol (FD NeuroTechnologies, Ellicott City, MD) (n = 4). Brains were sliced using a freezing-sliding microtome (Leica SM2000R) at a thickness of 150μm. Images of the CA1 and DG were taken with a Leica CTR5000 brightfield 63X oil objective, coded, and analyzed in a blinded manner using ImageJ software.

For hematoxylin and eosin staining, following transcardial perfusion with saline, brains from WT and Arf4$^{+/-}$ mice were fixed in 4% PFA-PBS for 48 hours, transferred to 70% ethanol, and embedded in paraffin. 5μm sagittal sections were cut for conventional hematoxylin and eosin staining.

BDNF immunohistochemistry was performed on 30 μm coronal WT and Arf4$^{+/-}$ brain sections following transcardial perfusion with saline and a 48 hour fixation in 4% PFA-PBS. Briefly, free-floating sections were treated with 3% H_2O_2 and 10% methanol in PBS to block endogenous peroxidase. The sections were incubated with PBS/10% normal donkey serum/1% milk/0.2% gelatin for 1 hour, followed by overnight incubation with primary anti-BDNF antibody (1:100, Santa Cruz Biotechnology). Sections were further processed using a biotinylated secondary donkey anti-rabbit antibody (1:1000, Jackson ImmunoResearch), avidin-peroxidase complex (ABC) and diaminobenzidine (DAB). The stained sections were mounted on slides, cleared with Xylene and coverslipped. Images were taken with a Leica CTR5000 brightfield 5X objective, and BDNF immunoreactivity was analyzed by densitometry using ImageJ software.

Electrophysiology. Two-month old mice were deeply anesthetized and euthanized following UCSF animal protocol guidelines. Then the brains were quickly removed and immersed in ice-cold cutting solution containing (in mM) 234 sucrose, 2.5 KCl, 1.25 NaH2PO4, 10 MgSO4, 26 NaCO3, 11 glucose and 1.3 ascorbic acid, and oxygenated with 95% O_2/5% CO_2. Transverse slices of 325 μm were cut on a Leica VS1000 vibroslicer (Leica, Germany) and incubated at 32°C for 30 min in an interface incubation chamber (Automated Scientific, CA), after which the slices continued to be incubated in

the same chamber at room temperature. For recording, slices were transferred to a submerged recording chamber and continuously perfused with oxygenated artificial cerebrospinal fluid (aCSF) containing (in mM) 126 NaCl, 2.5 KCl, 1.25 NaH2PO4, 1 MgSO4, 26 NaCO3, 10 glucose and 2 CaCl2 at 3mL/min (25°C). Whole-cell recordings were performed on visually identified dentate granule cells and fully matured granule cells were identified by input resistance (less than 400MΩ). To isolate miniature excitatory postsynaptic currents (mEPSCs), 100μM picrotoxin (Sigma), 5μM bicuculline (Tocris) and 0.5μM tetrodotoxin (Abcam) were added to the perfusate. The internal pipette solution contains (in mM) 120 CsMeSO3, 4 NaCl, 2 MgCl2, 10 HEPES, 5 EGTA, 5 MgATP, 0.3 Na_3GTP and 5 QX-314. Series resistance (<30MΩ) was constantly monitored and the recording was discarded if changes >15% occur. Data were digitized at 20 kHz by a Multiclamp 700A amplifier (Axon Instruments, Union City, CA) and acquired with a Digidata-1322A digitizer and WinLTP program (WinLTP Inc, University of Bristol, UK). Offline analysis was performed using Mini-analysis program (Synaptosoft inc) and the threshold setting for event detection was set at 4x the amplitude of baseline noise. Four hundred events were analyzed for each cell and only events recorded 10 minutes after whole cell break-in were included in the data analysis.

Behavioral tests. Behavioral testing was performed using male and female mice that were 4-5 months of age at the time of testing. All experiments and analyses were performed blind to genotype. The pattern separation test is used to measure an animal's ability to distinguish between similar events (Dere et al., 2007). Mice were habituated to the pattern separation testing room for one hour prior to training. During the training

period, mice were placed in an open chamber with a specific floor pattern and two identical objects, and were allowed to explore for 10 minutes. Following a 30-minute inter-trial interval, mice were placed in a second open chamber with a different floor pattern and two identical objects unique from the objects in the first trial. After 3 hours, mice were tested for 10 minutes in a chamber consisting of a floor pattern from either trial one or trial two, one object from trial one, and one object from trial two. The time each mouse spent exploring the object in the novel context (e.g., object from trial one in context from trial two) was compared with the time spent exploring the object in the old context. Exploration of an object was defined as the length of time a mouse's nose was 1 cm away from the object, and video recordings of the trials and test period were used to manually analyze exploration time.

For the Morris water maze test, the water maze pool (122 cm, diameter) was filled with opaque water (21ºC) and contained a submerged platform (10 cm, diameter) during hidden trials (Andrews-Zwilling et al., 2010; Harris et al., 2003). The ability of mice to locate the hidden platform was determined in two sessions (3.5 hours apart) per day for 5 days. Each session consisted of two 60 sec trials with a 15 min intertrial interval. The platform location remained constant during the hidden trials, and entry points were changed for each trial. The latency to reach the hidden platform was recorded as a measure of spatial learning. Probe trials (60 sec, platform removed) were performed 24, 72, and 120 hours after the hidden trials. Memory retention was measured by the percent time spent in the target quadrant compared to the average time spent in the other three quadrants, as well as by the number of crossings over the original position of the target platform compared to the number of crossings over the equivalent platform positions in

other quadrants. Following the probe trials, the ability of mice to locate a clearly visible platform was tested in three sessions (two trials/session) to exclude differences in vision and swim speed. Performance was monitored with an EthoVision video-tracking system (Noldus Information Technology).

The open field test is a standard test for general locomotor activity, willingness to explore, and anxiety (Crusio 2001). It consists of a square enclosure in which infrared detectors track animal movement. Locomotor and exploratory activity is assessed by the number of basic movements and rearings, whereas the proportion of time spent in the center of the enclosure is used as a measure of anxiety (Sahay et al., 2011). Mice were placed in the center of the chamber and were tested for 15 min.

The rotarod test, using a steady-speed rotarod set at 16RPM, was performed by placing mice on rotating drums and measuring each animal's latency to fall over a period of 300 seconds (Dunham et al., 1957).

The Elevated Plus Maze is a test for rodent anxiety and is based on a rodent's aversion to open spaces (File and Miya, 2001). The apparatus consists of two open arms and two enclosed arms at right angles to each other. Mice were placed on the central platform and were allowed to explore the apparatus for 10 minutes. Anxiety was assessed by comparing the amount of time spent in open versus enclosed arms.

Statistical analysis. Unless stated otherwise, all values are expressed as mean ± SEM. Statistical analyses were performed with GraphPad Prism software. Differences between the means were assessed by *t*-test or one factor ANOVA followed by a Bonferroni *post-*

hoc test. A *p*-value of <0.05 was considered to be statistically significant. Statistical values are denoted as follows: * $p < 0.05$, ** $p < 0.01$, *** $p < 0.001$.

CHAPTER 3

Arf4 Regulates Dentate Gyrus-Mediated Pattern Separation and Dendritic Spine Development

Arf4$^{+/-}$ mice have impairments in a DG-dependent pattern separation task. To study the roles of Arf4 *in vivo*, we used a gene-trapping strategy to try to generate Arf4$^{-/-}$ mice (Fig. 1A). Since Arf4$^{-/-}$ mice were embryonically lethal, we focused our *in vivo* studies on Arf4$^{+/-}$ mice. Arf4$^{+/-}$ mice were fertile, viable and showed no overt phenotype. Arf4 protein levels were reduced by 49% in the hippocampus of Arf4$^{+/-}$ mice compared to wildtype (WT) littermates (Fig. 1B). X-gal staining of 4.5-month-old Arf4$^{+/-}$ mice showed that Arf4 is highly expressed in the DG (Figs. 1C and D), prompting us to investigate the potential roles of Arf4 in DG-dependent memory tasks.

Since the DG is known to be involved in an animal's ability to distinguish between similar events (Schmidt et al., 2011), we asked whether the loss of one copy of Arf4 might affect performance in a pattern separation task. This task involved training mice to associate a certain environmental context with specific objects in two training sessions, followed by a testing session in which the rodents' ability to recognize context-object distinctions was analyzed. Whereas WT mice spent a greater proportion of time exploring the object in the novel context than the object in the familiar context, Arf4$^{+/-}$ mice showed no difference in the proportion of time spent with either object during the testing phase (Fig. 1E). Neither WT nor Arf4$^{+/-}$ mice showed significant differences in the amount of time spent with the two identical objects in either of the training sessions

(Figs. 1F and G). Thus, Arf4$^{+/-}$ mice were unable to effectively distinguish between two similar but unique situations. Interestingly, Arf4$^{+/-}$ mice did not show deficits in spatial learning (Fig. 2A) or memory retention (Figs. 2B and C), suggesting that the neurological impairments are specific to DG-dependent pattern separation. Arf4$^{+/-}$ mice were also not impaired in locomotor and exploratory activity (open field test) (Figs. 2D–F), motor coordination (rotarod) (Fig. 2G), or anxiety-related behaviors (elevated plus maze) (Figs. 2H and I).

FIGURE 1

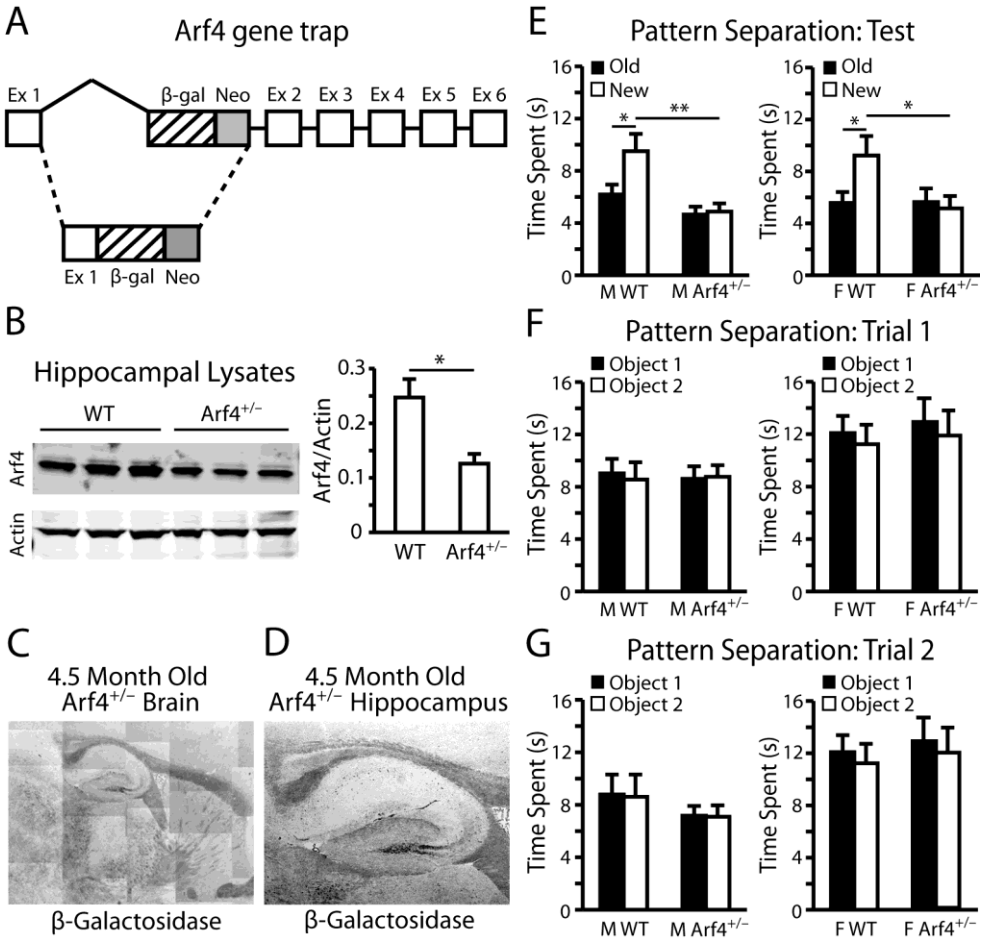

Figure 1. Arf4$^{+/-}$ mice are impaired in a dentate-gyrus dependent pattern separation task. All mice were between 4–5 months of age at the time of experimentation. (*A*) A

map of the Arf4 gene trapping construct obtained from BayGenomics (ES cell line CSH658). Ex, exon; β-gal, β-galactosidase gene; neo, neomycin-resistance gene. (*B*) Hippocampi from three WT and Arf4$^{+/-}$ littermate pairs were homogenized, followed by immunoblotting with anti-Arf4 (left panel). Actin loading controls are shown. Quantification of Arf4 protein levels in hippocampi prepared from WT or Arf4$^{+/-}$ mice (right panel). Arf4 protein levels were normalized to actin. (*C*) X-gal stained sagittal brain section from an Arf4$^{+/-}$ mouse at 5X magnification. (*D*) Representative image from a 4.5-month-old Arf4$^{+/-}$ hippocampus. (*E*) Quantification of the amount of time male (left panel) or female (right panel) WT and Arf4$^{+/-}$ mice spent exploring a novel object/context during a pattern separation task. (N = 12-13 mice per genotype per sex). (*F–G*) Quantification of the amount of time male (left panel) or female (right panel) WT and Arf4$^{+/-}$ mice spent exploring an object in a specific context during the first (*F*) or second (*G*) trial of the pattern separation task. All data are mean ± SEM. * $p < 0.05$, ** $p < 0.01$.

FIGURE 2

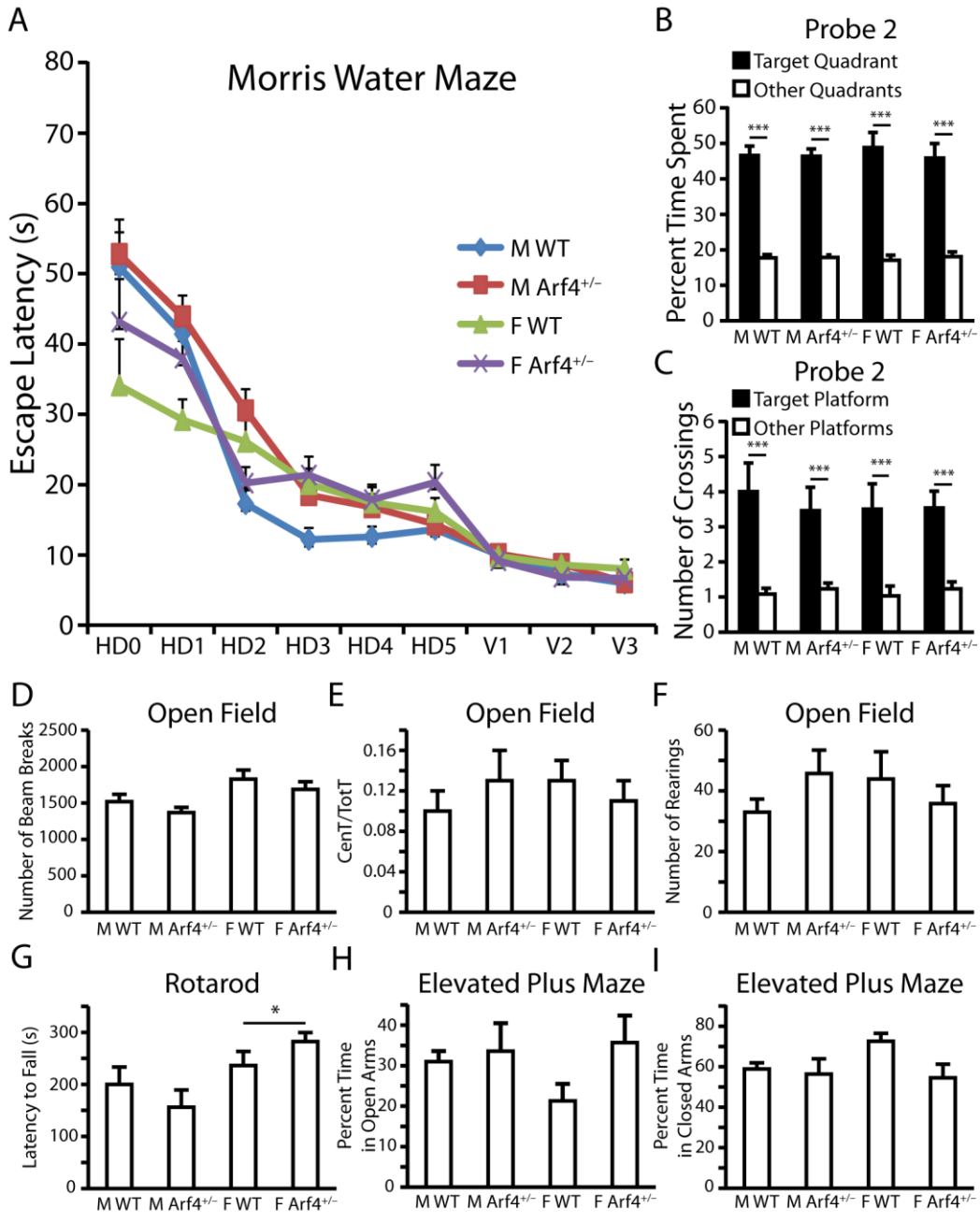

Figure 2. Arf4$^{+/-}$ mice are not impaired in spatial learning and memory, general locomotor activity, motor coordination, or anxiety behavior. Mice were 4–5 months of age at the time of experimentation (12–13 mice per genotype per sex). (*A*) Results

from Morris water maze test for spatial learning and memory. Graph of escape latency times. Points represent averages of daily trials. HD, hidden platform day (2 trials/session, 2 sessions/day); HD0, first trial on HD1; V, visible platform day (2 trials/session, 2 sessions/day). (*B*–*C*) Results from probe trials performed 72h after the final hidden platform training (Probe 2). Data are presented as percent time spent in the target quadrant versus the average time spent in the other quadrants (*B*) and number of crossings over the original position of the target platform compared to the number of crossings over the equivalent platform positions in other quadrants (*C*). (*D*–*F*) Results from open field test for general locomotor activity. Data are presented as the total number of infrared beam breaks over the 15-minute testing period (*D*), ratio of activity in the center of the open field compared to activity in the center plus the periphery (*E*), and total number of rearings over a 15 minute period (*F*). CenT, total number of beam breaks in the center; TotT, total number of beam breaks in the center plus periphery. (*G*) Rotarod test for motor coordination. Rotarod was set at 16RPM and animals were tested during three independent trials, each lasting a maximum of 300 seconds. The average latency to fall is shown over all three trials. (*H*–*I*) Results from elevated plus maze test for anxiety. Maze consists of two open arms and two closed arms. The percent time spent by male and female WT and $Arf4^{+/-}$ mice in the open (*H*) and closed (*I*) arms is shown. All data are mean ± SEM. * $p < 0.05$, *** $p < 0.001$.

Reduced spine density and mEPSC amplitude in $Arf4^{+/-}$ DG granule cells. The overall structures and morphologies of the hippocampus, cortex, and other brain regions appeared normal in $Arf4^{+/-}$ brains compared to controls, as determined by hematoxylin

and eosin staining (Fig. 3). We then examined the potential effects of Arf4 heterozygosity on neuronal fine structure using a modified Golgi-Cox staining protocol (Figs. 4A, 4B, and 5A). Both apical and basal dendrites of pyramidal neurons from the CA1 region (Fig. 4C), as well as dendrites from granule cells of the DG region (Fig. 5B), were analyzed (n = 4 mice/genotype). Although the CA1 region of $Arf4^{+/-}$ mice did not show spine density (Figs. 4B, C) or morphology (Fig. 4D) alterations compared with controls, there was a significant decrease in total spine density in the granule cells of the DG (Figs. 5A and B), as well as a decrease in mushroom spine density (Fig. 5C), which is in line with the high level expression of Arf4 in the DG (Figs. 1C and D). Furthermore, the amplitude of miniature excitatory postsynaptic currents (mEPSCs) was 37% lower in $Arf4^{+/-}$ DG granule cells than controls (Figs. 5D–F). The frequency of mEPSCs did not differ between the two genotypes (Figs. 5G and H). Thus, reducing Arf4 by 50% significantly impaired spine development and the electrophysiological function of granule cells in the DG.

FIGURE 3

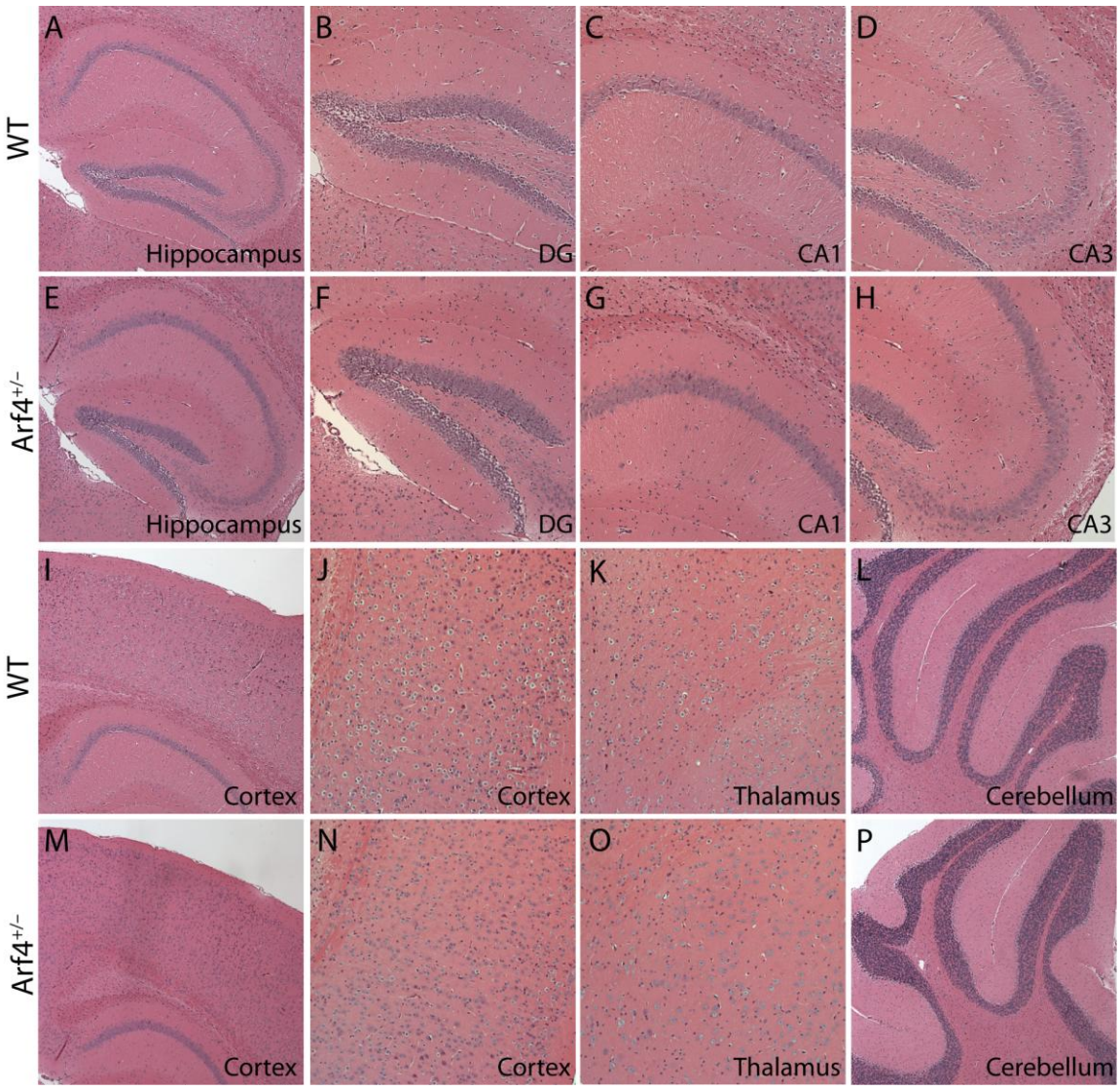

Figure 3. Overall structure and morphology of Arf4$^{+/-}$ brains are not altered compared to WT controls. (*A–P*) Hematoxylin and eosin-stained paraffin brain sections from WT and Arf4$^{+/-}$ mice. Representative images of the hippocampus (*A, E*), DG (*B, F*), CA1 (*C, G*), CA3 (*D, H*), cortex (*I, J, M, N*), thalamus (*K, O*), and cerebellum (*L, P*) from WT and Arf4$^{+/-}$ mice are shown.

FIGURE 4

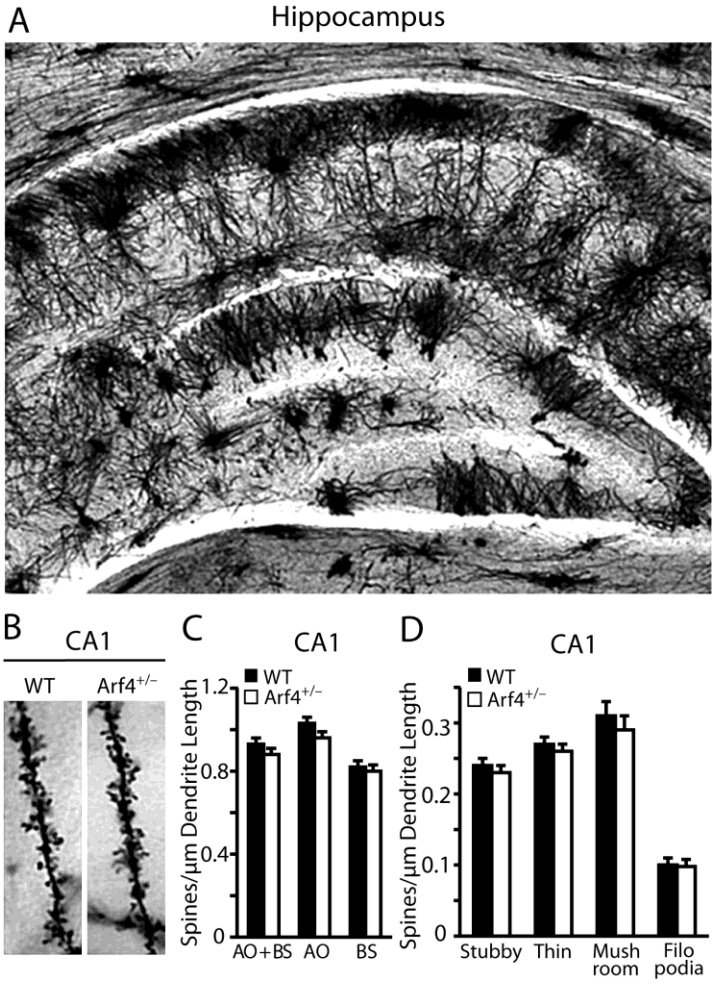

Figure 4. CA1 spine density is not altered in Arf4$^{+/–}$ mice compared to WT mice. (*A*) Golgi impregnation of a WT hippocampus at 5X. (*B*) Representative dendrites for CA1 pyramidal neurons of WT and Arf4$^{+/–}$ mice at 63X magnification. (*C*) Averaged total spine density in the CA1 region of WT and Arf4$^{+/–}$ mice (28–30 neurons/genotype). (*D*) Spine densities for specific spine subtypes in the CA1 region of WT and Arf4$^{+/–}$ mice.

FIGURE 5

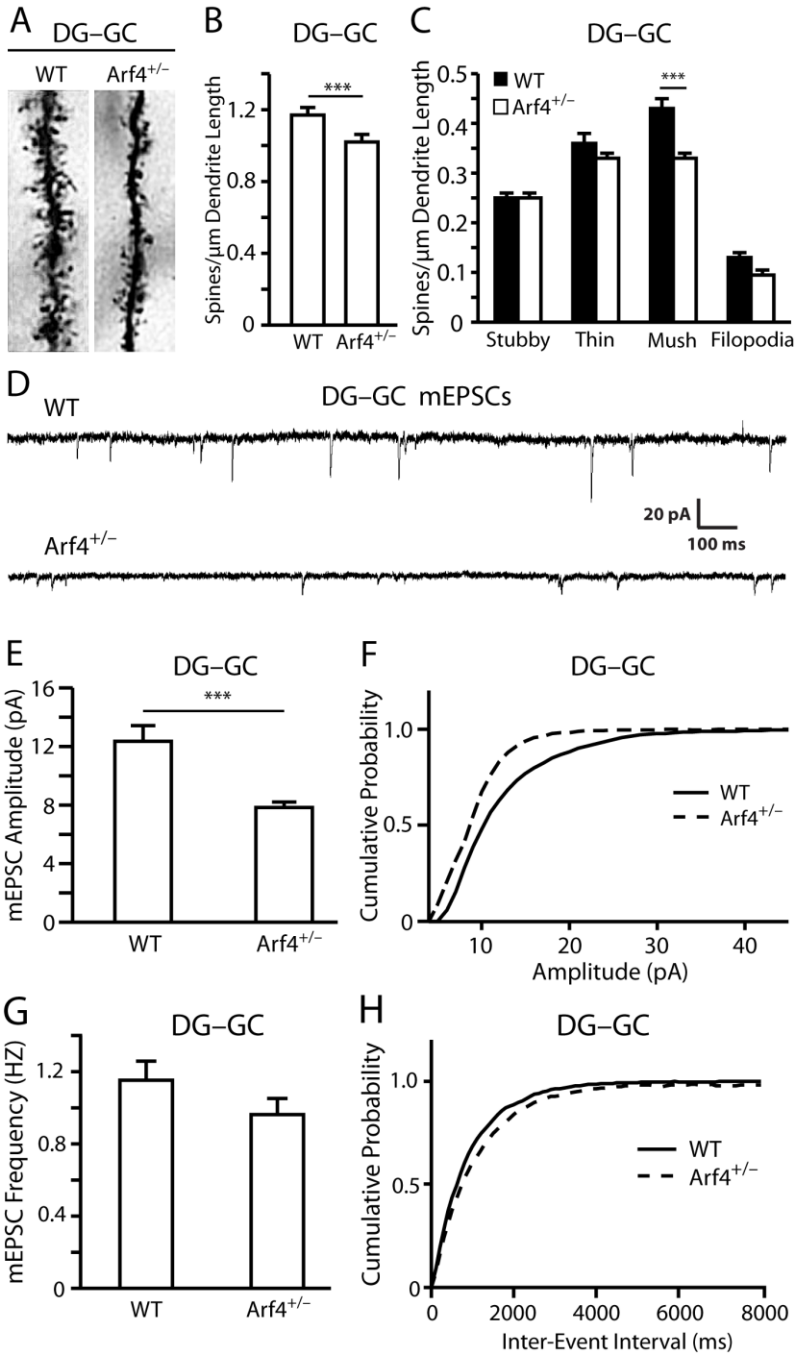

Figure 5. Decreased dendritic spine density and mEPSC amplitude in the DG of Arf4$^{+/-}$ mice compared to WT mice. (*A*) Representative dendrites for DG granule cells

of WT and Arf4$^{+/-}$ mice at 4 months of age (n = 4 mice/genotype). (*B*) Averaged total spine density per μm dendrite length in the dentate gyrus of WT and Arf4$^{+/-}$ mice (28–30 neurons/genotype). (*C*) Spine densities for specific spine subtypes in the DG of WT and Arf4$^{+/-}$ mice. (*D–F*) Electrophysiological recordings reveal a decrease in amplitude of mEPSCs in Arf4$^{+/-}$ (n = 9 cells) compared to WT controls (n = 6 cells) at 2 months of age. All data are mean ± SEM. * $p < 0.05$, ** $p < 0.01$, *** $p < 0.001$. (*G–H*) Spontaneous mEPSC frequency is not altered in Arf4$^{+/-}$ granule cells (n = 9 cells) compared to WT granule cells (n = 6 cells) at 2 months of age.

Arf4 is expressed in neurons and localizes to dendritic spines. Arf4 is expressed in the hippocampi of 4.5-month-old mice, as well as in primary neurons and Neuro-2a (N2a) neuroblastoma cells (Figs. 6A–C), as determined by western blots. When a HA- (Figs. 6D–F) or mCherry-tagged (Figs. 6G–I) form of human Arf4 was expressed in mouse primary neurons, Arf4 was visible throughout the soma and dendrites, including dendritic spines. Furthermore, both Arf4-HA and Arf4-mCherry co-localized with GFP-β-actin (Figs. 6D–I), which forms networks in dendritic spines (Hotulainen and Hoogenraad, 2010). These results point to a potential role for Arf4 in modulating neuronal function at the level of dendritic spines.

FIGURE 6

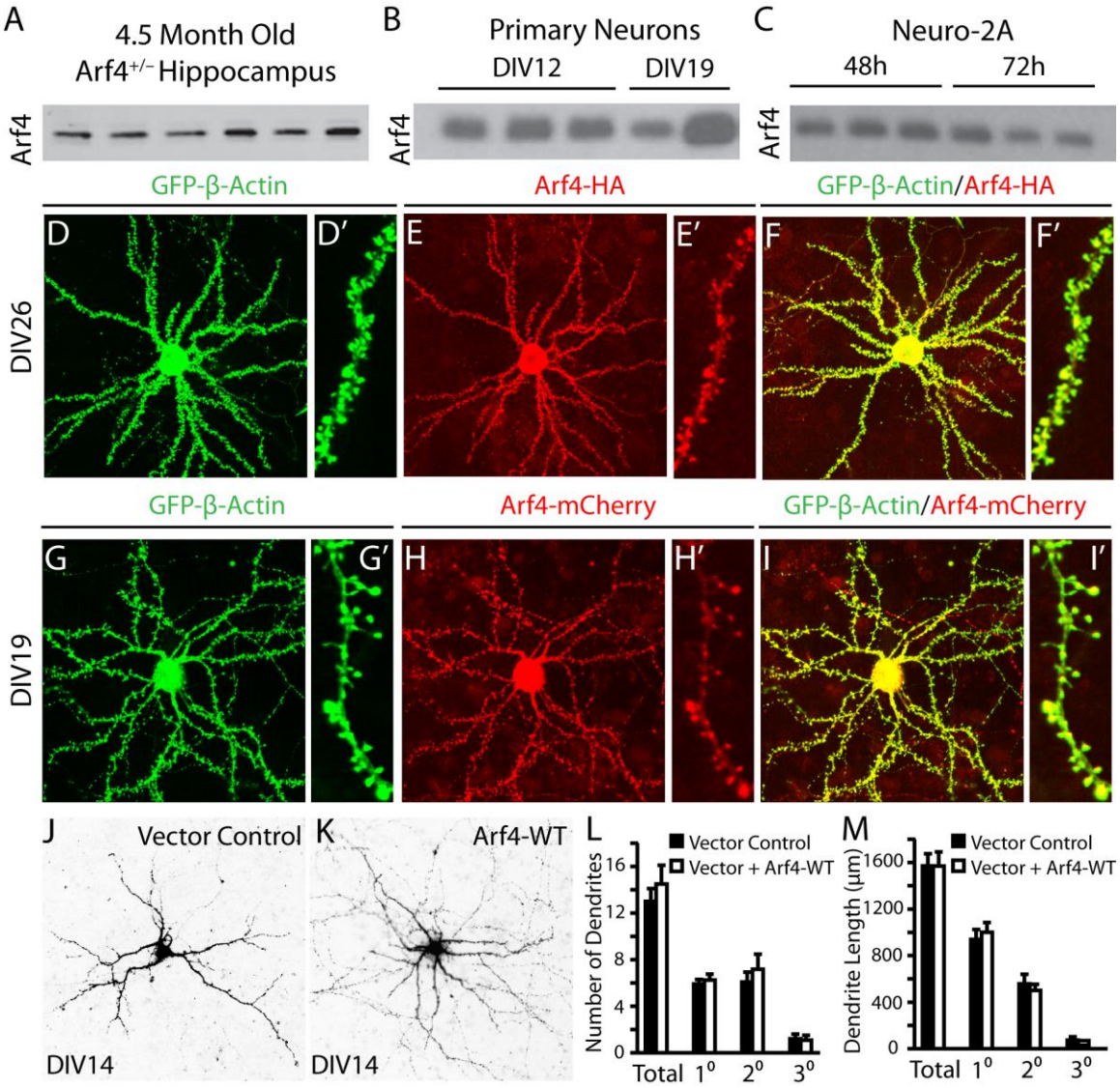

Figure 6. Expression of Arf4 in brain of 4.5-month-old mice and in primary neurons, and the effect of Arf4 overexpression on dendritic morphology. (*A*) Hippocampi from WT mice were prepared as described in methods, followed by immunoblotting with anti-Arf4 (n = 6). (*B*) Mixed hippocampal and cortical neurons were prepared from E18–E19 WT mouse embryos, and neuronal lysates were collected at DIV12 and DIV19. Samples were immunoblotted with anti-Arf4. (*C*) Lysates from WT

Neuro-2A cells were collected 48 and 72 hours after plating, followed by immunoblotting with anti-Arf4. (*D–I'*) Primary neuron co-transfected with GFP-β-actin and Arf4-HA (*D–F'*) or Arf4-mCherry (*G–I'*) at DIV5 and imaged at DIV14. Higher (*D–I*) and lower (*D'–I'*) magnification images are shown. *(J, K)* Representative images of dendrite morphology for neurons transfected with a control vector (*J*) or vector plus Arf4-WT (*K*). (*L, M*) The number (*L*) and length (*M*) of primary, secondary, and tertiary dendrites were quantified. (n = 12 neurons per experimental condition). All data are mean ± SEM.

Arf4 promotes dendritic spine development in primary neuronal cultures. To examine whether Arf4 regulates spine development, we transfected cultured primary mouse cortical and hippocampal neurons at 5 days *in vitro* (DIV5) with cDNA constructs encoding either human Arf4-HA and GFP-β-actin or GFP-β-actin alone. Overexpression of GFP-β-actin does not impair neuronal function or dendritic spine morphology and density and can, therefore, be used to highlight dendritic spines for imaging and quantification (Moore et al., 2007; Morales et al., 2000). Overexpression of Arf4 did not significantly alter total dendrite number or length, nor did it change the number or length of primary, secondary, or tertiary dendrites (Figs. 6J–M). However, Arf4 overexpression dramatically increased dendritic spine density at DIV12 (Figs. 7B and B′), DIV14 (Figs. 7D and D'), and DIV19 (Figs. 7F and F') compared with control neurons at each time point (Figs. 7A, C, and E). Furthermore, this increase in spine density was significant across time points, whereas spine densities remained relatively constant throughout development for neurons transfected with GFP-β-actin alone (Fig. 7G). We observed

similar increases in spine density in GFP-β-actin co-transfection experiments using Arf4-mCherry in the place of Arf4-HA.

The physiological effects of small GTPases depend on whether they are in a functionally active (GTP-bound) or inactive (GDP-bound) state (Donaldson and Jackson, 2011). To address the effect of Arf4 activity on spine density and morphology, we expressed a series of Arf4 functional mutants in cultured neurons. The Arf4 mutants used included the constitutively active mutant Arf4-Q71L, which remains bound to GTP, and the inactive mutant Arf4-T31N, which remains GDP-bound (Kim et al., 2003; Woo et al., 2009). Arf4-Q71L had an even more pronounced effect on stimulating spine development than wildtype Arf4, whereas Arf4-T31N did not enhance spine development compared with controls (Figs. 8A and B). Arf4 and its active mutant also promoted stubby and thin spine development (Fig. 8C). Overexpression of the inactive Arf4-T31N mutant significantly reduced mushroom spine density, suggesting that restricting Arf4 to its GDP-bound state prevents the development of mature spines.

FIGURE 7

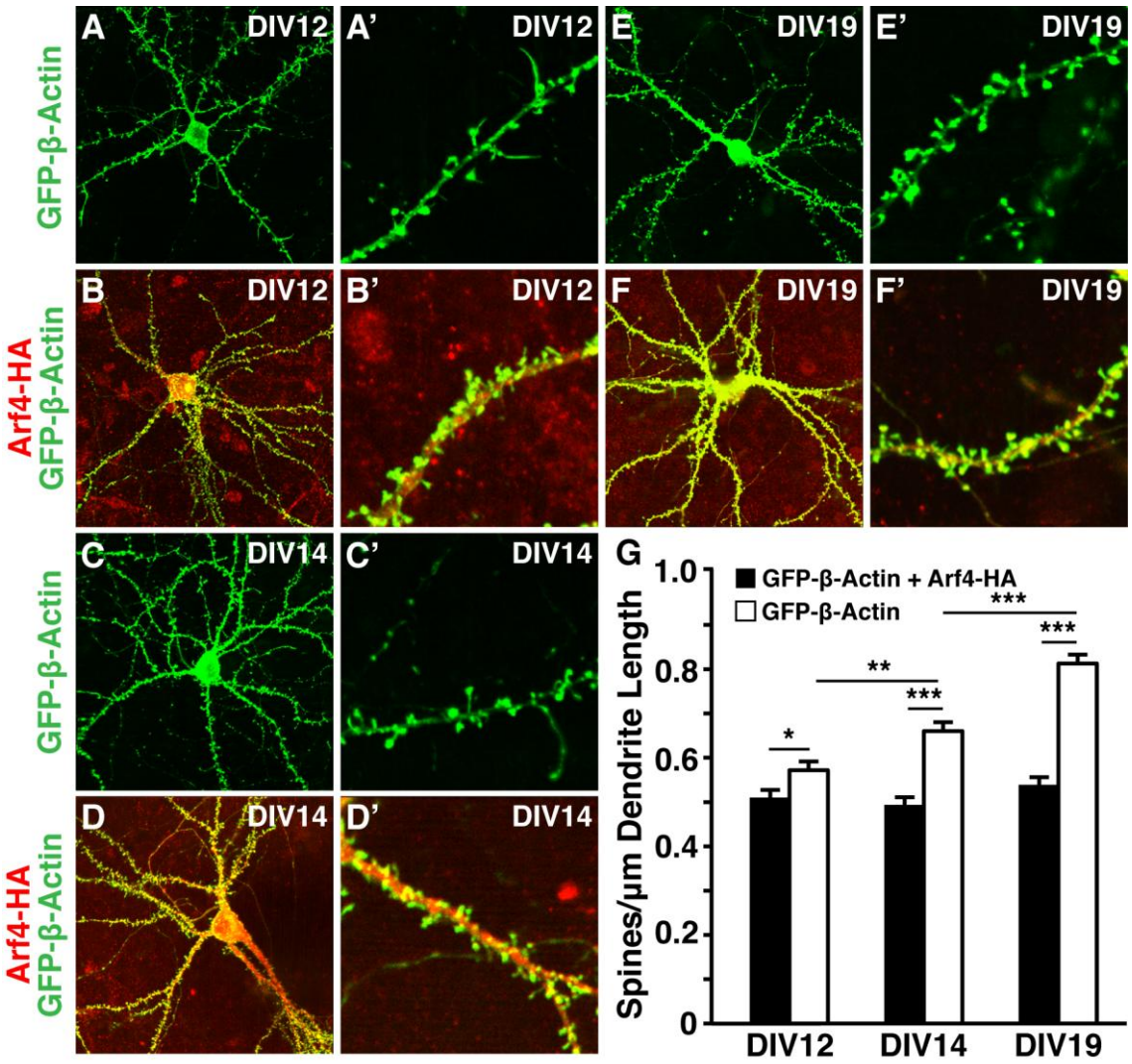

Figure 7. Arf4 overexpression promotes dendritic spine development in mouse primary neurons. (*A–B'*) Neurons transfected with GFP-β-actin alone (*A–A'*) or together with Arf4-HA (*B–B'*) at DIV5 and imaged at DIV12 (n = 9–10 neurons). (*C–D'*) Neurons transfected with GFP-β-actin alone (*C–C'*) or together with Arf4-HA (*D–D'*) at DIV5 and imaged at DIV14 (n = 8–10 neurons). (*E–F'*) Neurons transfected with GFP-β-actin alone (*E–E'*) or together with Arf4-HA (*F–F'*) at DIV5 and imaged at DIV19 (n = 8–9 neurons). (*G*) Averaged spine density of neurons transfected with GFP-β-actin alone or

with GFP-β-actin plus Arf4-HA at several time points. All data are mean ± SEM. * $p < 0.05$, ** $p < 0.01$, *** $p < 0.001$.

FIGURE 8

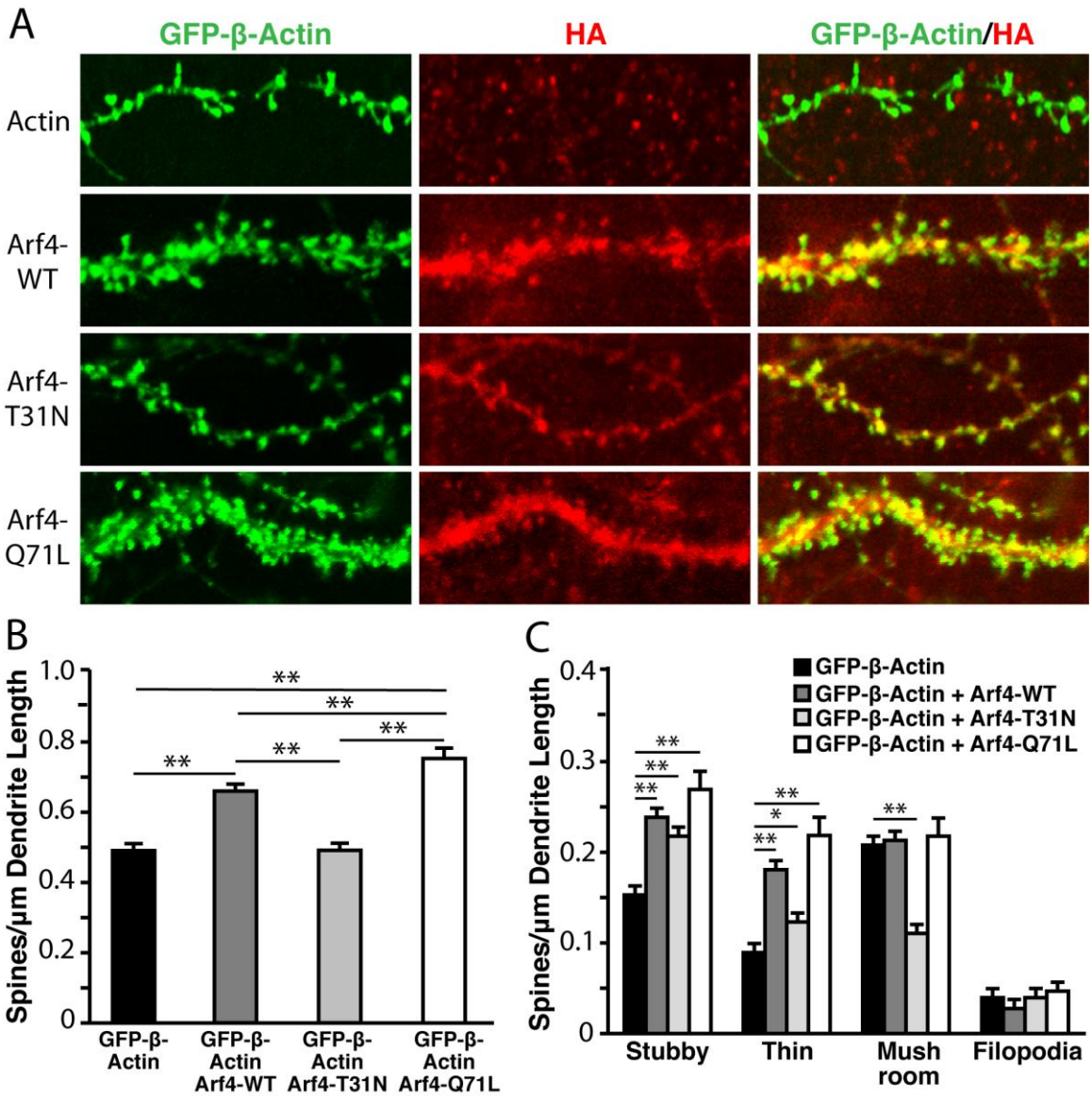

Figure 8. Overexpression of constitutively active Arf4 (Arf4-Q71L) promotes dendritic spine development to a greater extent that Arf4-WT. (A) Primary hippocampal and cortical neurons were cotransfected at DIV5 with GFP-β-actin plus Arf4-HA [wild-type (WT), T31N, or Q71L] and analyzed at DIV14 (n = 8–13 neurons).

(*B–C*) Quantification of the effect of Arf4 and its mutants on total spine density (*B*) and the densities of specific spine subtypes (*C*) following transfection with Arf4 or its mutants. All data are mean ± SEM. * $p < 0.05$, ** $p < 0.01$.

Arf4 is required for normal spine development. We next asked whether the absence of endogenous Arf4 perturbs spine development. We transfected neurons at DIV5 with a FUGW2-based vector encoding GFP and one of two mouse Arf4-short hairpin RNA (shRNA) sequences, and then imaged the cells at DIV14. Both Arf4-shRNA1 and Arf4-shRNA2 markedly decreased Arf4 protein levels in Neuro-2a cells 48 hours post-transfection (Figs. 9A and B). Knockdown of Arf4 significantly decreased total spine density (Figs. 9D–E') as well as the individual densities of all spine subtypes except filopodia (Fig. 9H), compared to controls (Figs. 9C and C'). To verify the target specificity of Arf4-shRNA, we co-expressed human Arf4-HA—whose expression is resistant to mouse shRNA knockdown—with mouse Arf4-shRNA. Expression of human Arf4-HA completely rescued the effects on spine density (Figs. 9F and G) and morphology (Fig. 9H) caused by endogenous mouse Arf4 knockdown, demonstrating the specificity of Arf4-shRNA's effects.

FIGURE 9

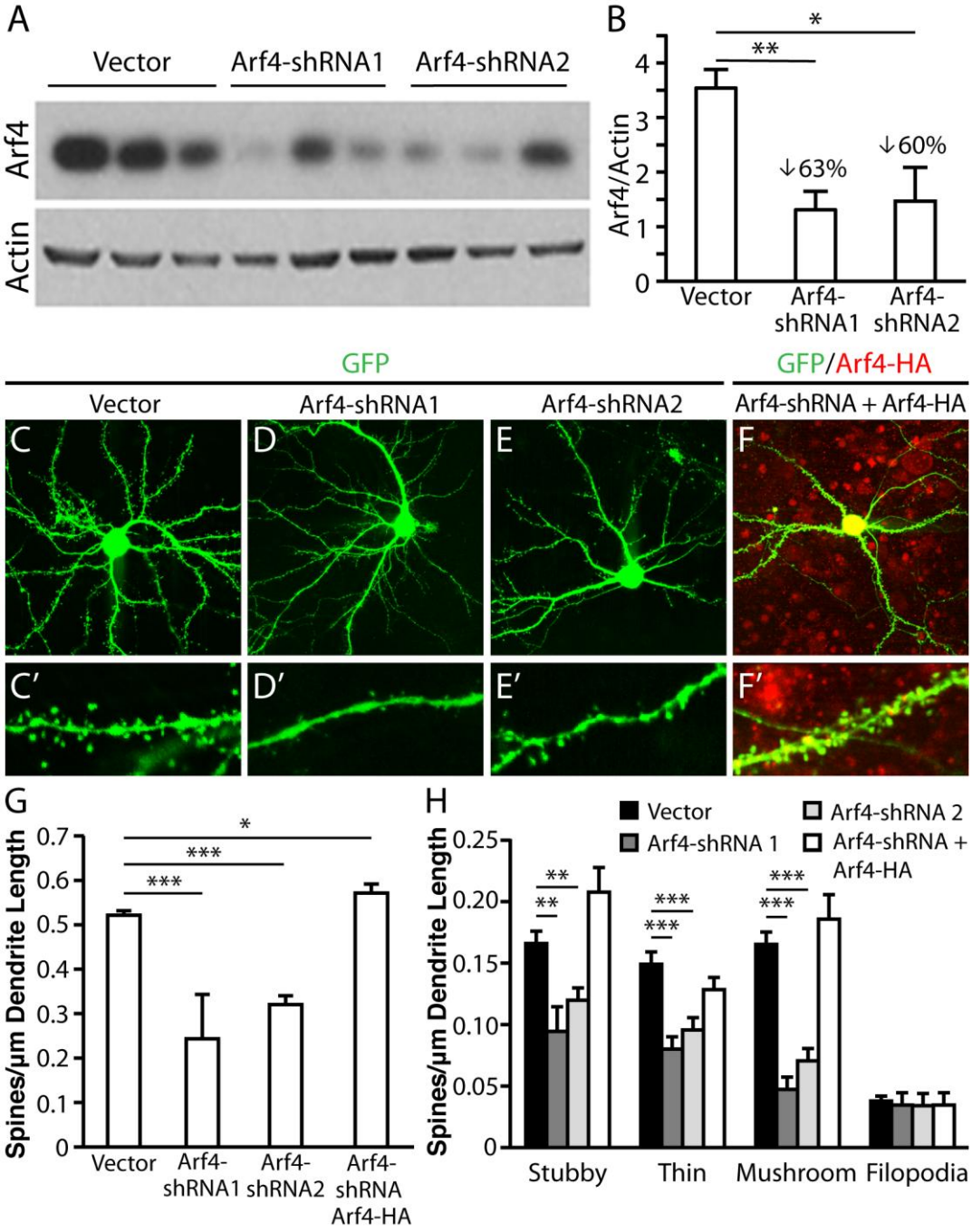

Figure 9. Knockdown of Arf4 by shRNA reduces spine density in mouse primary neurons. (*A*) To verify the efficacy of the Arf4 shRNA-encoding plasmid, mouse Neuro-2A cells were transfected with Arf4-shRNA1 or Arf4-shRNA2 and equal protein

amounts of transfected cell lysates were analyzed by immunoblotting with α-Arf4 antibody, or with α-actin antibody as a control. (*B*) Quantification of knockdown efficacy by Arf4-shRNA1 or Arf4-shRNA2 in mouse Neuro-2A cells. Arf4 levels are normalized to actin. (*C–F'*) Representative examples of WT neurons transfected with FUGW2-GFP plasmid (*C–C'*), Arf4-shRNA1 (*D–D'*), Arf4-shRNA2 (*E–E'*), or Arf4-shRNA plus Arf4-HA (rescue) (*F–F'*). Lower (*C–F*) and higher (*C'–F'*) magnification images are shown (N = 7–13 neurons per condition). (*G*) Total spine and (*H*) spine subtype densities from each of the experimental conditions. All data are mean ± SEM. * $p < 0.05$, ** $p < 0.01$, *** $p < 0.001$.

ASAP1, an Arf4 GAP, negatively regulates spine development. Previous studies have shown that ASAP1 functions as an Arf4 GAP and forms a complex with Arf4 (Mazelova et al., 2009). We found that overexpressed ASAP1 is localized to dendrites and dendritic spines in mouse primary neurons, similar to Arf4 (Figs. 10B and B'). Neurons transfected at DIV5 with ASAP1-Flag, together with FUGW2-GFP for visualization of spines, showed a significant decrease in total spine density (Figs. 10B, B', and E) as well as in stubby and mushroom spine density at DIV14 (Fig. 10F). To determine whether the spine-promoting effect of Arf4 is regulated by ASAP1, we co-transfected primary neurons with ASAP1-Flag and either Arf4-HA-WT or constitutively active Arf4-HA-Q71L, together with FUGW2-GFP. Both WT (Figs. 10C and C') and constitutively active (Figs. 10D and D') Arf4 partially blocked ASAP1-induced changes in spine density and morphology, suggesting that ASAP1 is a negative regulator of Arf4's effects on spine density.

FIGURE 10

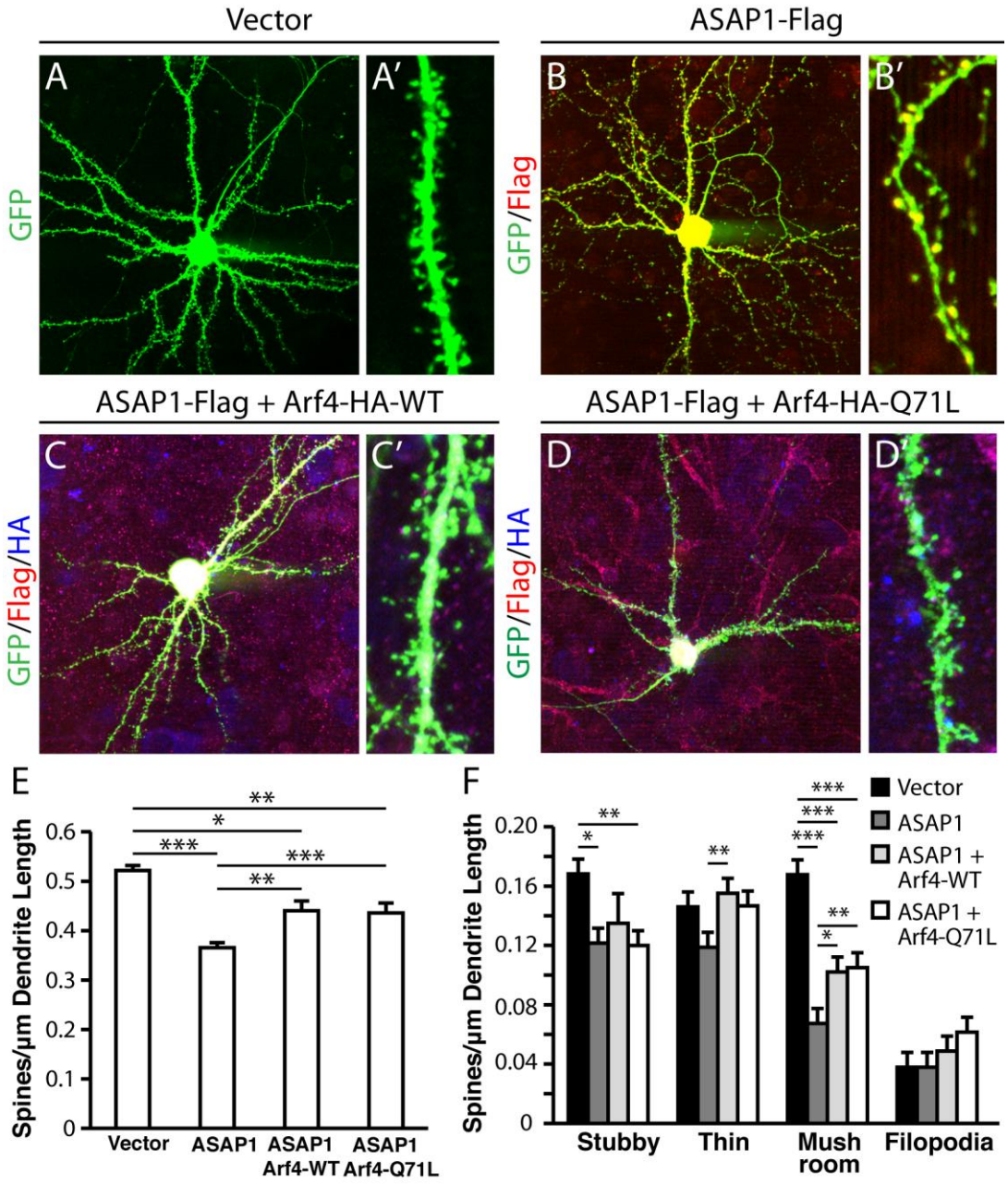

Figure 10. ASAP1, an Arf4 GAP, inhibits dendritic spine formation, and both Arf4-WT and Arf4-Q71L partially rescue this inhibition. (*A–D'*) Representative examples of WT neurons transfected at DIV5 with FUGW2-GFP plasmid alone (*A, A'*), or together

with ASAP1-Flag (*B, B'*), ASAP1-Flag plus Arf4-WT-HA (*C, C'*), or ASAP1-Flag plus Arf4-HA Q71L (*D, D'*) and analyzed at DIV14. Lower (*A–D*) and higher (*A'–D'*) magnification images are shown. (n = 11-13 neurons per condition). (*E–F*) Quantification of the effect of ASAP1 alone or together with Arf4-HA-WT or Arf4-HA-Q71L on dendritic spine density (*E*) and morphology (*F*). All data are mean ± SEM. * $p < 0.05$, ** $p < 0.01$, *** $p < 0.001$.

BDNF levels are not altered in Arf4$^{+/-}$ mice or in Arf4-overexpressing primary neurons. Since brain-derived neurotrophic factor (BDNF) plays critical roles in both pattern separation (Beckinschtein et al., 2011) and dendritic spine development (Vigers et al., 2012; Kaneko et al., 2012), we asked whether BDNF expression might be altered in Arf4$^{+/-}$ mice. We found that BDNF protein levels in the CA1, CA3, and DG regions of the hippocampus were similar in Arf4$^{+/-}$ mice compared to their wildtype littermates (Fig. 11A–C). BDNF levels also remained unaltered in Arf4-overexpressing neurons compared to neurons not overexpressing Arf4 (Fig. 11D–F). Thus, Arf4 levels do not appear to have a direct effect on neuronal BDNF expression *in vitro* or *in vivo*.

FIGURE 11

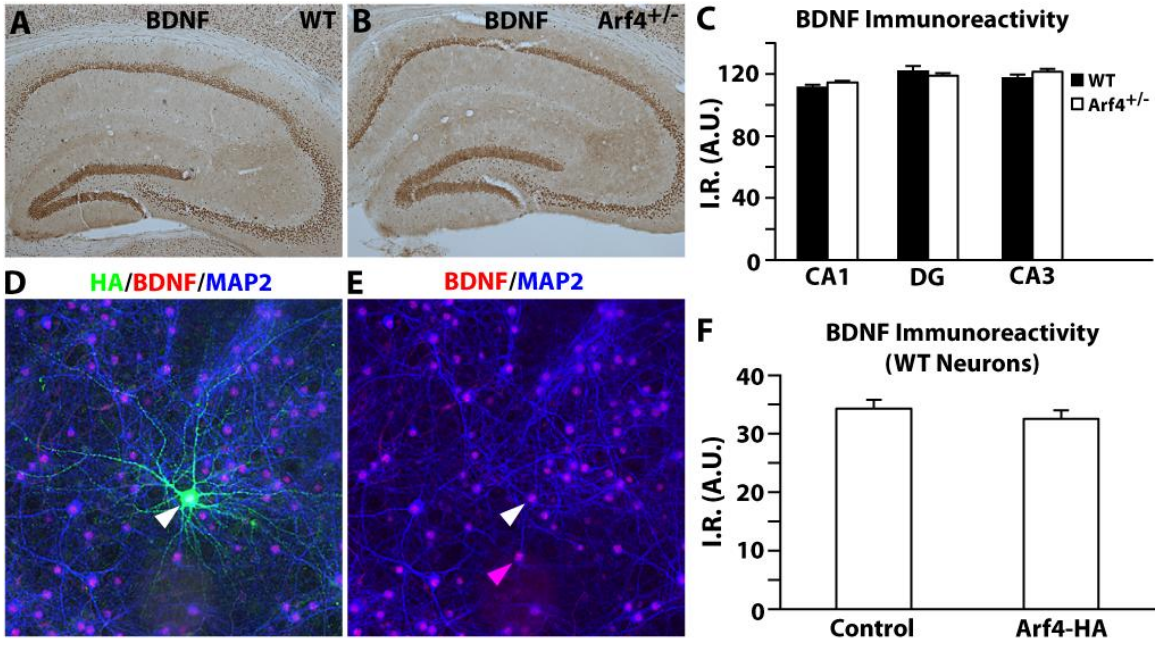

Figure 11. Arf4 levels do not affect BDNF expression *in vivo* or *in vitro.* *(A–B)* Representative images of WT (A) and Arf4$^{+/-}$ (B) hippocampi stained for BDNF, followed by DAB development. *(C)* Quantification of BDNF immunoreactivity in the hippocampus (n = 3 mice per genotype). *(D–E)* Duplicate images of primary neurons transfected with Arf4-HA at DIV5 and stained with HA (green), BDNF (red), and MAP2 (blue) antibodies at DIV14. Arrows point to a neuron overexpressing Arf4-HA (white arrow) or a neuron that does not overexpress Arf4-HA (pink arrow) *(F)* Quantification of BDNF expression in primary neurons either overexpressing or not overexpressing human Arf4-HA (n = 15 neurons per condition). A.U. = arbitrary units.

Arf4 overexpression rescues spine loss in neurons from an AD-related apoE4 mouse model. We next examined Arf4's role in spine development in the context of a neurodegenerative disease model. We investigated the possibility that Arf4 might rescue

apoE4-caused spine loss in neurons from transgenic mice expressing apoE4 selectively in neurons [neuron-specific enolase (NSE)-apoE4]. These mice have impairments in learning and memory (Raber et al., 1998), as well as a loss of dendritic spines in primary neurons and in the hippocampus and cortex (Brodbeck et al., 2011). We found that Arf4 mRNA levels were significantly reduced in hippocampi from 10-month-old female NSE-apoE4 (vs. NSE-apoE3) mice (36% reduction, $p = 0.015$). Furthermore, Arf4 protein levels were also significantly reduced in primary neurons from NSE-apoE4 mice compared to those from NSE-apoE3 mice (Figs. 12A and B).

Consistent with previous findings (Brodbeck et al., 2011), the dendritic spine density of NSE-apoE4 neurons (Figs. 12E and E') was significantly less than that of either NSE-apoE3 (Figs. 12D and D') or WT neurons (Figs. 12C and C'). Additionally, NSE-apoE4 neurons had fewer stubby, thin, and mushroom spines compared with WT neurons (Fig. 12J). Overexpression of Arf4 fully restored the spine loss observed in NSE-apoE4 neurons (Figs. 12H and H'). Furthermore, Arf4 overexpression increased spine density to an extent similar to that observed in Arf4-overexpressing WT (Figs. 12F and F') and NSE-apoE3 neurons (Figs. 12G and G'). The apoE4-induced decrease in specific spine subtypes was also rescued by Arf4 overexpression (Fig. 12J).

FIGURE 12

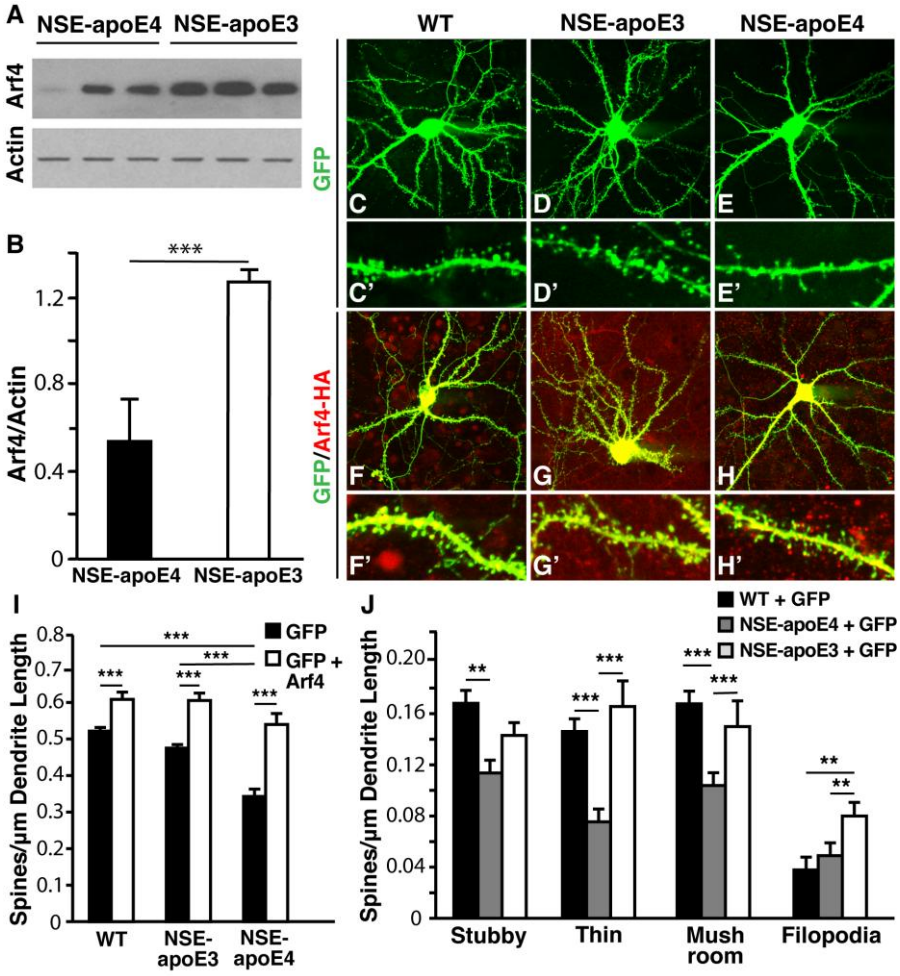

Figure 12. Arf4 overexpression rescues spine loss in apoE4-expressing primary neurons. (*A*) Representative Western blot of actin and Arf4 levels in NSE-apoE4 and NSE-apoE3 mice reveal a decrease in Arf4 protein levels from NSE-apoE4 mice compared to those from NSE-apoE3 mice. Primary neuron lysates were prepared in triplicate, and actin was used as a loading control. (*B*) Quantification of the ratio of Arf4/Actin levels. Data are mean ± SD. * $p < 0.05$, *** $p < 0.001$. (*C–H'*) Primary hippocampal and cortical neurons were cultured from WT, homozygous NSE-apoE3, or homozygous NSE-apoE4 mouse E18–E19 embryos. Neurons were transfected with

FUGW2 plasmid alone (for visualization of spines) or with FUGW2 plus Arf4-HA-WT at DIV5 and analyzed at DIV14. Lower (*C–H*) and higher (*C'–H'*) magnification images are shown. (*C–E'*) WT (*C–C'*), NSE-apoE3 (*D–D'*), or NSE-apoE4 (*E–E'*) neurons transfected with empty FUGW2 plasmid (n = 12–13 neurons). (*F–H'*) WT (*F–F'*), NSE-apoE3 (*G–G'*), or NSE-apoE4 (*H–H'*) neurons cotransfected with FUGW2 plus Arf4-HA-WT (n = 8–12 neurons). (*I*) Quantification of total spine densities for each experimental condition. (*J*) Spine subtype densities for each experimental condition. All data are mean ± SEM. * $p < 0.05$, ** $p < 0.01$, *** $p < 0.001$.

CHAPTER 4

Conclusions and Discussion

In this study, we show that the small GTPase Arf4 is a novel modulator of DG-dependent pattern separation tasks by regulating dendritic spine development. The loss of one copy of Arf4 *in vivo* leads to severe impairments in pattern separation, as well as a decrease in DG granule cell spine density and mEPSC amplitude. In primary neuron cultures, overexpression of wildtype Arf4 promotes spine development even at an early stage (DIV12), whereas shRNA knockdown of Arf4 inhibits it. These effects are partially mediated by ASAP1, an Arf4 GAP. In addition, overexpression of Arf4 rescues the dendritic spine loss caused by apoE4, the major genetic risk factor for AD. These results indicate that Arf4, by promoting spine development, represents a useful target for treatments of neurodegenerative diseases that cause profound synaptic loss, such as AD.

Arf4 regulates dendritic spine density and morphology. Spine number and structural plasticity are tightly correlated with synaptic function in the mammalian brain (Tada and Sheng, 2006; Kasai et al., 2003). We found that Arf4 overexpression promotes spine development, particularly that of thin spines. Previous studies have shown that thin spines are more transient and motile than mushroom spines, and an increase in the proportion of thin spines represents a greater capacity to stabilize after LTP (Holtmaat et al., 2005; Zuo et al., 2005). Mushroom spines have larger postsynaptic densities (PSDs) and more glutamate receptors than thin spines, making the synapse functionally stronger and more

stable (Bourne and Harris, 2007; Tada and Sheng, 2006). We found that knocking down Arf4 decreases thin and mushroom spine density and, consistently, impairs the electrophysiological function of granule cells of the dentate gyrus. Decreases in both spine types have been reported in animal models of cognitive decline (Dumitriu et al., 2010; Perez-Cruz et al., 2011). Based on these results, a significant loss of both transient thin spines and stable mushroom spines in primary neurons lacking Arf4 raises the possibility that Arf4 might be critical for both dendritic spine plasticity and stability.

Our study uncovered potential molecular mechanisms governing the effects of Arf4 on spine density and morphology. First, we found that the effects of Arf4 on spine development are related to its activity state. The GTP-bound form of Arf4 stably associates with intracellular organelle membranes and can activate downstream effectors (Woo et al., 2009; Duijsings et al., 2009). By constitutively binding to GTP, Arf4-Q71L likely activates signaling pathways that can induce spine morphogenesis to a greater extent than wildtype Arf4. In contrast, Arf4-T31N remains bound to GDP and is therefore theoretically inactive. Previous studies have reported seemingly contradictory roles for GDP-bound Arf proteins (Arf-T31N) as either inactive mutants whose physiological effects do not differ from wildtype Arfs (Chen and Shields, 1996; Islam et al., 2007), or as dominant-negative mutants with inhibitory effects on vesicular transport and other cellular functions (Dascher and Balch, 1994). Interestingly, our results suggest that Arf4-T31N acts as an inactive mutant with respect to its effects on total spine density, but displays some dominant-negative characteristics by specifically reducing the density of mushroom spines.

Small GTPases modulate actin cytoskeletal rearrangement and dynamics in both neuronal and non-neuronal cells (Hotulainen and Hoogenraad, 2010), suggesting that actin-binding proteins or their regulators might serve as effectors of Arf4 in spine morphogenesis. We found that the Arf GAP ASAP1 negatively regulates dendritic spine density compared to controls, and this effect is partially rescued by co-expression of ASAP1 together with Arf4-WT. ASAP1 is known to regulate the actin cytoskeleton (Randazzo et al., 2000), indicating that Arf4 and ASAP1 might interact to influence spine cytoskeletal dynamics. Recent studies have shown that Arf activation promotes recruitment of several actin-regulatory proteins, including cortactin and dynamin, to the vesicle-budding sites of the trans-Golgi network (TGN) (Cao et al., 2005; Carreno et al., 2004). Our finding that Arf4 colocalizes with actin in primary neurons suggests a potential interplay between Arf4 and actin-regulating proteins in dendritic spines.

Role of Arf4 in dentate gyrus-dependent pattern separation tasks. Mossy fiber "detonator" synapses arising from DG granule cells strongly activate the CA3 region and are involved in a variety of neurological functions, including memory and spatial representations (Yassa and Stark, 2011; Palmer and Good, 2011). Our experiments showed that Arf4 heterozygosity *in vivo* leads to reductions in spine number and mEPSC amplitude in the DG, and these alterations accompany profound pattern separation impairments. These results indicate that Arf4 could serve as a novel regulator of the mossy fiber pathway by regulating granule cell spine development and electrophysiological activity.

Spine head size is positively correlated with mEPSC amplitude (Matsuzaki et al., 2001), and the functional loss of NMDA receptors in DG granule cells has been associated with impairments in pattern separation (McHugh et al., 2007). In our study, mushroom spine numbers were significantly lower in the DG of Arf4$^{+/-}$ compared to WT mice, and this spine loss correlated with a reduction in mEPSC amplitude. Mushroom spines contain more AMPA and NMDA receptors than other spine types, and these receptors are critical for strengthening synaptic connections (Bourne and Harris, 2007). Therefore, the context recognition impairments seen in Arf4$^{+/-}$ mice could be related to reduced granule cell-specific synaptic communication caused by the loss of mushroom-type spines.

Arf4 overexpression as a potential therapeutic strategy for AD-related spine loss. As spine loss is strongly correlated with cognitive impairments in AD (Penzes et al., 2011; Terry et al., 1991), a potential therapeutic strategy for restoring cognitive function in AD patients could be to increase dendritic spine density, thereby strengthening synaptic connections. In our current study, we found that overexpression of Arf4 restored spine loss in NSE-apoE4 neurons. Thus, increasing Arf4's function might serve as a potential therapeutic strategy for restoring impairments in spine development and synaptic connectivity.

The preclinical period prior to the diagnosis of AD is characterized by deficits in a number of memory-related processes, including pattern separation (Palmer and Good, 2011; Salmon, 2012). Patients with amnestic mild cognitive impairment (MCI), for instance, showed an impaired ability to distinguish between a previously seen object and

a very similar but unobserved object (Yassa et al., 2010). Some aged rodents that do not develop AD pathology nevertheless have memory deficits, such as a failure to encode novel information while navigating similar situations (Wilson et al., 2004). In our current study, it is intriguing that young (4–5 month old) $Arf4^{+/-}$ mice have pattern separation deficits that are similar to those found in pre-clinical MCI patients and aged rodents, but exhibit normal spatial learning and memory. The $Arf4^{+/-}$ mouse model might therefore represent a unique tool to investigate early cognitive dysfunctions prior to the onset of AD pathology. Our studies should provide further understanding of the molecular mechanisms underlying DG-dependent memory tasks and spine development, and how these processes are degraded in neurodegenerative disorders, such as AD.

CHAPTER 5

Future Studies

To further examine the molecular mechanisms underlying Arf4's effects on dendritic spine development. Our study showed that ASAP1, an Arf GAP that shows GTPase activity toward Arf4 (Mazelova et al., 2009), regulates Arf4's effects on dendritic spine development. Although an Arf4 GEF has not yet been identified, GBF1 has emerged as a potential candidate based on a co-immunoprecipitation study (Szul et al., 2007). A [^{35}S] GTPγS binding assay can be used to determine whether GBF1 promotes the exchange of Arf4-GDP for Arf4-GTP. If GBF1 does show GEF activity toward Arf4, GBF1 can be overexpressed in neurons either alone or together with Arf4 to assess its involvement in Arf4's regulation of spine density and morphology.

The downstream effectors of Arf proteins include phospholipid metabolizing enzymes such as PIP kinase (PIPK) γ and phospholipase (PLD) 2, which aid in actin cytoskeletal rearrangement of dendritic spines (Myers and Casanova, 2008; Donaldson and Jackson, 2011). Arf-GTP activates PLD2, which leads to an increase in PIP2 levels and the subsequent activation of actin regulatory proteins (Myers and Casanova, 2008). To determine whether PLD2 mediates Arf4's effects on spines, lenti-PLD2-shRNA can be used to knock down PLD2 in Arf4-overexpressing and control neurons, followed by quantification of spine density and morphology. PIPKIγ activity in Arf4-overexpressing neurons can be assayed by measuring levels of PI(4,5)P_2, the product of PIP phosphorylation by PIPKIγ (Wenk et al., 2001). The potential effect of PIPKIγ on Arf4-

mediated spine development can then be investigated by knocking down PIPKIγ in Arf4-overexpressing or control neurons using a lenti-PIPKIγ-shRNA construct.

To examine whether Arf4$^{+/-}$ mice exhibit altered pattern completion. The current study demonstrated that Arf4$^{+/-}$ mice are severely impaired in pattern separation at 4–5 months of age. Nakashiba et al reported that transgenic mice with normal or enhanced pattern separation exhibit impairments in another hippocampal process called pattern completion, which refers to the retrieval of complete memories from partial cues and is largely mediated by the CA3 region (Nakashiba et al., 2012). These and other findings (O'Reilly and McClelland, 1994; Toni et al., 2008) suggest a degree of trade-off or competition between pattern separation and pattern completion, which likely maintains an optimal balance between these two mnemonic processes.

A modified, partial-cue version of the Morris water maze (Nakazawa et al., 2002) can be used to examine whether Arf4$^{+/-}$ mice show altered pattern completion abilities compared to their wildtype controls. In this protocol, mice are first subjected to the full-cue, hidden platform version of the Morris water maze to assess their spatial reference memory. After the last probe trial, mice undergo an additional block of training (4 trials), followed by another probe trial in which three out of the four extramaze cues are removed from the walls. The ability of the mice to retrieve a memory from partial cues can then be assessed by measuring the amount of time spent searching for the phantom platform, as well as the number of crossings over the original location of the platform.

To investigate whether Arf4 overexpression can rescue apoE4-induced spine loss and learning and memory impairments *in vivo*. We found that Arf4 restores apoE4-

induced dendritic spine loss in primary neuronal cultures. To investigate the effects of Arf4 on apoE4-induced spine loss *in vivo*, a mCherry-tagged Arf4 lentivirus or vehicle can be injected into the hippocampi of NSE-apoE3 and NSE-apoE4 mice, and spine density and morphology of hippocampal neurons can then be examined by Golgi-Cox staining. Fluorescent immunostaining can also be used to compare levels of synaptic proteins, such as synapsin, bassoon, and PSD-95. To determine whether Arf4 overexpression can rescue apoE4-induced spatial learning and memory impairments, NSE-apoE3 and NSE-apoE4 mice injected with Arf4 lentivirus or vehicle can be tested for spatial learning and memory using the Morris water maze. Alternatively, neuron-specific transgenic Arf4-overexpressing mice can be generated and crossed with NSE-apoE4 mice to assess whether Arf4 overexpression can enhance cognitive function and rescue apoE4-caused learning and memory deficits.

References

Aimone JB, Deng W, Gage FH (2011) Resolving new memories: a critical look at the dentate gyrus, adult neurogenesis, and pattern separation. Neuron 70:589–596.

Andrews-Zwilling Y, Bien-Ly N, Xu Q, Li G, Bernardo A, Yoon SY, Zwilling D, Yan TX, Cheng L, Huang Y (2010) Apolipoprotein E4 causes age-and tau-dependent impairment of GABAergic interneurons, leading to learning and memory deficits in mice. J Neurosci 30: 13707–13717.

Beckinschtein P, Oomen CA, Saksida LM, Bussey TJ (2011) Effects of environmental enrichment and voluntary exercise on neurogenesis, learning and memory, and pattern separation: BDNF as a critical variable? Semin Cell Dev Biol 22:536–542.

Bhatt HD, Zhang S, Wen-Biao Gan (2009) Dendritic spine dynamics. Annu Rev Physiol 71:261–282.

Bourne J and Harris KM (2007) Do thin spines learn to be mushroom spines that remember? Curr Opin Neurobiol 17:381–386.

Brodbeck J, Balestra ME, Saunders AM, Roses AD, Mahley RW, Huang Y (2008) Rosiglitazone increases dendritic spine density and rescues spine loss caused by apolipoprotein E4 in primary cortical neurons. Proc Natl Acad Sci USA 105:1343–1346.

Brodbeck J, McGuire J, Liu Z, Meyer-Franke A, Balestra ME, Jeong DE, Pleiss M, McComas C, Hess F, Witter D, et al. (2011) Structure dependent impairments of intracellular apolipoprotein E4 trafficking and its detrimental effects are rescued by small-molecule structure correctors. J Biol Chem 286:17217–17226.

Brown MT, Andrade J, Radhakrishna H, Donaldson JG, Cooper JA, Randazzo PA (1998) ASAP1, a phospholipid-dependent Arf GTPase-activating protein that associates with And is phosphorylated by Src. Mol Cell Biol 18:7038–7051.

Burgess N, Maguire EA, O'Keefe J (2002) The human hippocampus and spatial and episodic memory. Neuron 35:625–641.

Cajal SR (1888) Estructura de los centros nerviosos de las aves. Rev Trim Histol Norm Patol 1:1–10.

Calabrese B, Wilson MS, Halpain S (2006) Development and regulation of dendritic spine synapses. Physiology (Bethesda) 21:38–47

Cao H, Weller S, Orth JD, Chen J, Huang B, Chen JL, Stamnes M, McNiven MA. (2005) Actin and Arf1-dependent recruitment of a cortactin-dynamin complex to the Golgi regulates post-Golgi transport. Nat Cell Biol 7:483–492.

Carreno S, Enggvist-Goldstein AE, Zhang CX, McDonald KL, Drubin DG (2004) Actin

dynamics coupled to clathrin-coated vesicle formation at the trans-Golgi network. J Cell Biol 165:781–788.

Casanova JE (2007) Regulation of Arf activation: the Sec7 family of guanine nucleotide exchange factors. 8:1476–1485.

Caselli RJ (2009) Age-related memory decline and apolipoprotein E e4. Discov Med 8:47–50

Chen J, Zhou Y, Mueller-Steiner S, Chen LF, Kwon H, Yi S, Mucke L, Gan L (2005) SIRT1 protects against microglia-dependent amyloid-beta toxicity through inhibiting NF kappaB signaling. J Biol Chem 280:40364–403674.

Chen YG and Shields D (1996) ADP-ribosylation factor-1 stimulates formation of nascent secretory vesicles from the trans-Golgi network of endocrine cells. J Biol Chem 271:5297–5300.

Choi S, Ko J, Lee JR, Lee HW, Kim K, Chung HS, Kim H, Kim E (2006) ARF6 and EFA6A regulate the development and maintenance of dendritic spines. J Neurosci 26:4811–4819.

Chun J, Shapovalova Z, Dejgaard SY, Presley JF, Melancon P (2008) Characterization of class I and II ADP-ribosylation factors (Arfs) in live cells: GDP-bound class II Arfs

associate with the ER-Golgi intermediate compartment independently of GBF1. Mol Biol Cell 19:3488–3500.

Cingolani LA and Goda Y (2008) Actin in action: the interplay between the actin cytoskeleton and synaptic efficacy. Nat Rev Neurosci 9:344–356.

Crusio WE (2001) Genetic dissection of mouse exploratory behavior. Behav Brain Res 125: 127–132.

Csepanyi-Komi R, Levay M, Liget E (2012) Small G proteins and their regulators in cellular signaling. Mol Cell Endocrinol 353:10–20.

Dascher C and Balch WE (1994) Dominant inhibitory mutants of ARF1 block endoplasmic reticulum to Golgi transport and trigger disassembly of the Golgi apparatus. J Biol Chem 269:1437–1448.

Dere E, Huston JP, De Souza Silva MA (2007) The pharmacology, neuroanatomy and neurogenetics of one-trial object recognition in rodents. Neurosci Biobehav Rev 31:673–704.

Donaldson JG and Jackson CL (2011) ARF family G proteins and their regulators: roles in membrane transport, development and disease. Nat Rev Mol Cell Biol 12:362–375.

D'Souza-Schorey C and Chavrier P (2006) ARF proteins: roles in membrane traffic and beyond. Nat Rev Mol Cell Biol 7:347–358

Duijsings D, Lanke KH, van Dooren SH, van Dommelen MM, Wetzels R, de Mattia F, Wessels E, van Kuppeveld FJ (2009) Differential membrane association properties and regulation of class I and class II Arfs. Traffic 10:316–323.

Dumanis SB, Tesoriero JA, Babus LW, Nguyen MT, Trotter JH, Ladu MJ, Weeber EJ, Turner RS, Xu B, Rebeck GW, et al. (2009) ApoE4 decreases spine density and dendritic complexity in cortical neurons in vivo. J Neurosci 29:15317–15322.

Dumitriu D, Hao J, Hara Y, Kaufmann J, Janssen WG, Lou W, Rapp PR, Morrison JH (2010) Selective changes in thin spine density and morphology in monkey prefrontal cortex correlate with aging related cognitive impairment. J Neurosci 30:7507–7515.

Dunham NW and Miya TS (1957) A note on a simple apparatus for detecting neurological deficit in rats and mice. J Am Pharm Assoc Am Pharm Assoc 46:208–209.
Fiala JC, Spacek J, Harris KM (2002) Dendritic spine pathology: cause or consequence of neurological disorders? Brain Res Rev 29:29–54.

File SE (2001) Factors controlling measures of anxiety and responses to novelty in the mouse. Behav Brain Res 125:151–157.

Gartner U, Alpar A, Behrbohm J, Heumann R, Arendt T (2005) Enhanced Ras activity promotes spine formation in synRas mice neocortex. Neuroreport 16:149–152

Gilbert PE, Kesner RP, Lee I (2001) Dissociating hippocampal subregions: double dissociation between dentate gyrus and CA1. Hippocampus 11:626–636.

Gillingham AK and Munro S (2007) The small G proteins of the Arf family and their regulators. Annu Rev Cell Dev Biol 23:579–611.

Gong Y and Lippa CF (2010) Review: disruption of the postsynaptic density in Alzheimer's disease and other neurodegenerative dementias. Am J Alzheimers Dis Other Demen 25: 547–555.

Harris FM, Brecht WJ, Xu Q, Tesseur I, Kekonius L, Wyss-Coray T, Fish JD, Masliah E, Hopkins PC, Scearce-Levie K, et al. (2003) Carboxyl-terminal truncated apolipoprotein E4 causes Alzheimer's disease-like neurodegeneration and behavioral deficits in transgenic mice. Proc Natl Acad Sci USA 100:10966–10971.

Henze DA, Wittner L, Buzsaki G (2002) Single granule cells reliably discharge targets in the hippocampal CA3 network in vivo. Nat Neurosci 5:790–795.

Hering H and Sheng M (2003) Activity-dependent redistribution and essential role of

cortactin in dendritic spine morphogenesis. J Neurosci 23:11759–11769.

Holtmaat AJ, Trachtenberg JT, Wilbrecht L, Shepherd GM, Zhang X, Knott GW, Svoboda K. (2005) Transient and persistent dendritic spines in the neocortex in vivo. Neuron 45:279–291.

Hotulainen P and Hoogenraad CC (2010) Actin in dendritc spines: connecting dynamics to function. J Cell Biol 189:619–627.

Islam A, Shen X, Hiroi T, Moss J, Vaughan M, Levine SJ. (2007) The brefeldin A inhibited guanine nucleotide-exchange protein, BIG2, regulates the constitutive release of TNFR1 exosome-like vesicles. J Biol Chem 282:9591–9599.

Ivanov A, Esclapez M, Pellegrino C, Shirao T, Ferhat L (2009) Drebrin A regulates dendritic spine plasticity and synaptic function in mature cultured hippocampal neurons. J Cell Sci 122:524–534.

Jang SY, Jang SW, Ko J (2012) Regulation of ADP-ribosylation factor 4 expression by small leucine zipper protein and involvement in breast cancer cell migration. Cancer Lett 314:185–197.

Jaworski J (2007) ARF6 in the nervous system. Eur J Cell Biol 86:513–524.

Ji Y, Gong Y, Gan W, Beach T, Holtzman DM, Wisniewski T. (2003) Apolipoprotein E isoform specific regulation of dendritic spine morphology in apolipoprotein E transgenic mice and Alzheimer's disease patients. Neuroscience 122:305–315.

Jung MW and McNaughton BL. (1993) Spatial selectivity of unit activity in the hippocampal granular layer. Hippocampus 3:165–182.

Kaneko M, Xie Y, An JJ, Stryker MP, Xu B (2012) Dendritic BDNF synthesis is required for late-phase spine maturation and recovery of cortical responses following sensory deprivation. J Neurosci 32:4790–4802.

Kasai H, Matsuzaki M, Noguchi J, Yasumatsu N, Nakahara H (2003) Structure-stability function relationships of dendritic spines. Trends Neurosci 26:360–368.

Kim SW, Hayashi M, Lo JF, Yang Y, Yoo JS, Lee JD (2003) ADP-ribosylation factor 4 small GTPase mediates epidermal growth factor receptor-dependent phospholipase D2 activation. J Biol Chem 278:2661–2668.

Knobloch M and Mansuy IM (2008) Dendritic spine loss and synaptic alterations in Alzheimer's disease. Mol Neurobiol 37:73–82.

Kropff E and Treves A. (2007) Uninformative memories will prevail: the storage of correlated representations and its consequences. HFSP J 1:249–262.

Lebeda RA and Haun RS (1999) Cloning and characterization of the human ADP-ribosylation factor 4 gene. Gene 237:209–214.

Lippman J and Dunaevsky A (2005) Dendritic spine morphogenesis and plasticity. J Neurobiol 64: 47–57.

Marr D (1971) Simple memory: a theory for archicortex. Philos Trans R Soc Lond B Biol Sci 262:23–81.

Matsuzaki M, Ellis-Davies GC, Nemoto T, Miyashita Y, Iino M, Kasai H (2001) Dendritic spine geometry is critical for AMPA receptor expression in hippocampal CA1 pyramidal neurons. Nat Neurosci 4:1086–1092.

Mazelova J, Astuto-Gribble L, Inoue H, Tam BM, Schonteich E, Prekeris R, Moritz OL, Randazzo PA, Deretic D. (2009) Ciliary targeting motif VxPx directs assembly of a trafficking module through Arf4. EMBO J 28:183–192.

McClelland JL, McNaughton BL, O'Reilly RC. (1995) Why are there complementary learning systems in the hippocampus and neocortex: insights from the successes and failures of connectionist models of learning and memory. Psychol Rev 102:419–457.

McHugh TJ, Jones MW, Quinn JJ, Balthasar N, Coppari R, Elmquist JK, Lowell BB,

Fanselow MS, Wilson MA, Tonegawa S. (2007) Dentate gyrus NMDA receptors mediate rapid pattern separation in the hippocampal network. Science 317:94–99.

Moore CD, Thacker EE, Larimore J, Gaston D, Underwood A, Kearns B, Patterson SI, Jackson T, Chapleau C, Pozzo-Miller L, et al. (2007) The neuronal Arf GAP centaurin alpha1 modulates dendritic differentiation. J Cell Sci 120:2683–2693.

Morales M, Colicos MA, Goda Y (2000) Actin-dependent regulation of neurotransmitter release at central synapses. Neuron 27:539–550.

Morris AM, Churchwell JC, Kesner RP, Gilbert PE (2012) Selective lesions of the dentate gyrus produce disruptions in place learning for adjacent spatial locations. Neurobiol Learn Mem 97:326–331.

Myers KR and Casanova JE (2008) Regulation of actin cytoskeleton dynamics by Arf-family GTPases. Trends Cell Biol 18:184–192.

Nakashiba T, Cushman JD, Pelkey KA, Renaudineau S, Buhl DL, McHugh TJ, Rodriguez Barrera V, Chittajallu R, Iwamoto KS, McBain CJ, et al. (2012) Young dentate granule cells mediate pattern separation, whereas old granule cells facilitate pattern completion. Cell 149:1–14.

Nakayama AY, Harms MB, Luo L (2000) Small GTPases Rac and Rho in the maintenance of dendritic spines and branches in hippocampal pyramidal neurons. J Neurosci 20:5329–5338.

Nakazawa K, Quirk MC, Chitwood RA, Watanabe M, Yeckel MF, Sun LD, Kato A, Carr CA, Johnston D, Wilson MA, et al. (2002) Requirement for hippocampal CA3 NMDA receptors in associative memory recall. Science 297:211–218.

Nie Z, Hirsch DS, Randazzo PA (2003) Arf and its many interactors. Curr Opin Cell Biol 15:396–404.

Norman KA and O'Reilly RC (2003) Modeling hippocampal and neocortical contributions to recognition memory: a complementary-learning-systems approach. Psychol Rev 110:611–646

O'Keefe J and Dostrovsky J (1971) The hippocampus as a spatial map. Preliminary evidence from unit activity in the freely-moving rat. Brain Res 34:171–175.

O'Reilly RC and McClelland JL (1994) Hippocampal conjunctive encoding, storage, and recall: avoiding a trade-off. Hippocampus 4:661–682.

Palmer A and Good M (2011) Hippocampal synaptic activity, pattern separation and episodic like memory: implications for mouse models of Alzheimer's disease pathology.

Biochem Soc Trans 39:902–909.

Peebles CL, Yoo J, Thwin MT, Palop JJ, Noebels JL, Finkbeiner S. (2010) Arc regulates spine morphology and maintains network stability in vivo. Proc Natl Acad Sci USA 107:18173–18178.

Penzes P, Cahil ME, Jones KA, VanLeeuwen JE, Wolfrey KM (2011) Dendritic spine pathology in neuropsychiatric disorders. Nat Neurosci 14:285–292.

Penzes P and Vanleeuwen JE (2011) Impaired regulation of synaptic actin cytoskeleton in Alzheimer's disease. Brain Res Rev 67:184–192.

Perez-Cruz C, Nolte MW, van Gaalen MM, Rustay NR, Termont A, Tanghe A, Kirchhoff F, Ebert U. (2011) Reduced spine density in specific regions of CA1 pyramidal neurons in two transgenic mouse models of Alzheimer's disease. J Neurosci 31:3926 3934.

Raber J, Wong D, Buttini M, Orth M, Bellosta S, Pitas RE, Mahley RW, Mucke L. (1998) Isoform-specific effects of human apolipoprotein E on brain function revealed in ApoE knockout mice: increased susceptibility of females. Proc Natl Acad Sci USA 95:10914–10919.

Randazzo PA, Andrade J, Miura K, Brown MT, Long YQ, Stauffer S, Roller P, Cooper

JA. (2000) The Arf GTPase activating protein ASAP1 regulates the actin cytoskeleton. Proc Natl Acad Sci USA 97:4011–4016.

Randazzo PA and Hirsch DS (2004) Arf GAPs: multifunctional proteins that regulate membrane traffic and actin remodeling. Cell Signal 16:401–413.

Roses AD (1996) Apolipoprotein E alleles as risk factors in Alzheimer's disease. Annu Rev Med 47:387–400.

Sahay A, Scobie KN, Hill AS, O'Carroll CM, Kheirbek MA, et al. (2011) Increasing adult hippocampal neurogenesis is sufficient to improve pattern separation. Nature 472:466–473.

Sakagami H, Sanda M, Fukaya M, Miyazaki T, Sukegawa J, Yanagisawa T, Suzuki T, Fukunaga K, Watanabe M, Kondo H. (2008) IQ Arf4GEF/BRAG1 is a guanine nucleotide exchange factor for Arf6 that interacts with PSD-95 at postsynaptic density of excitatory synapses. Neurosci Res 60:199–212.

Salmon DP (2012) Neuropsychological features of mild cognitive impairment and preclinical Alzheimer's disease. Curr Top Behav Neurosci 10:187–212.

Schmidt B, Marrone DF, Markus EJ (2011) Disambiguating the similar: the dentate gyrus and pattern separation. Behav Brain Res 226:56–65.

Segal M (2005) Dendritic spines and long-term plasticity. Nat Rev Neurosci 6:277–284.

Sekino Y, Kojima N, Shirao T (2007) Role of actin cytoskeleton in dendritic spine morphogenesis. Neurochem Int 51:92–104.

Strittmatter WJ, Saunders AM, Schmechel D, Pericak-Vance M, Enghild J, Salvesan GS, Roses AD (1993) Apolipoprotein E: high-avidity binding to beta-amyloid and increased frequency of type 4 allele in late-onset familial Alzheimer disease. Proc Natl Acad Sci U S A 90:1977–1981.

Suzuki I, Owada Y, Suzuki R, Yoshimoto T, Kondo H (2001) Localization of mRNAs for six ARFs (ADP-ribosylation factors) in the brain of developing and adult rats and changes in the hypoglossal nucleus after its axotomy. Mol Brain Res 88:124–134.

Tackenberg C, Ghori A, Brandt R (2009) Thin, stubby or mushroom: spine pathology in Alzheimer's disease. Curr Alzheimer Res 6:261–268.

Tada T and Sheng M (2006) Molecular mechanisms of dendritic spine morphogenesis. Curr Opin Neurobiol 16:95–101.

Tashiro A, Minden A, Yuste R (2000) Regulation of dendritic spine morphology by the rho family of small GTPases: antagonistic roles of Rac and Rho. Cereb Cortex 10:927

938.

Terry RD, Masliah E, Salmon DP, Butters N, DeTeresa R, Hil R, Hansen LA, Katzman R. (1991) Physical basis of cognitive alterations in Alzheimer's disease: synapse loss is the major correlate of cognitive impairment. Ann Neurol 30:572–580.

Toner CK, Pirogovsky E, Kirwan CB, Gilbert PE (2009) Visual object pattern separation deficits in nondemented older adults. Learn Mem 16:338–342.

Toni N, Laplagne DA, Zhao C, Lombardi G, Ribak CE, Gage FH, Schinder AF (2008) Neurons born in the adult dentate gyrus form functional synapses with target cells. Nat Neurosci 11:901–907.

Treves A, Tashiro A, Witter ME, Moser EI (2008) What is the mammalian dentate gyrus good for? Neuroscience 154:1155–1172.

Vanderklish PW and Edelman GE (2002) Dendritic spines elongate after stimulation of group metabotropic glutamate receptors in cultured hippocampal neurons. Proc Natl Acad Sci 99:1639–1644.

Vigers AJ, Amin DS, Talley-Farnham T, Gorski JA, Xu B, Jones KR (2012) Sustained expression of brain-derived neurotrophic factor is required for maintenance of dendritic spines and normal behavior. Neuroscience 212:1–18.

Wenk MR, Pellegrini L, Klenchin VA, Di Paolo G, Chang S, Daniell L, Arioka M, Martin TF, De Camilli P (2001) PIP kinase Igamma is the major PI(4,5)P(2) synthesizing enzyme at the synapse. Neuron 32:79–88.

Wennerberg K, Rossman KL, Der CJ (2005) The Ras superfamily at a glance. J Cell Sci 118:843–846.

Wilson IA, Ikonen S, Gureviciene I, McMahan RW, Gallagher M, Eichenbaum H, Tanila H. (2004) Cognitive aging and the hippocampus: how old rats represent new environments. J. Neurosci 24:3870–3878.

Woo IM, Eun SY, Jang HS, Kang ES, Kim GH, Kim HJ, Lee JH, Chang KC, Kim JH, Han CW, et al. (2009) Identification of ADP ribosylation factor 4 as a suppressor of N-(4 hydroxyphenyl) retinamide-induced cell death. Cancer Letters 276:53–60.

Wu GY, Deisseroth K, Tsien RW (2001) Spaced stimuli stabilize MAPK pathway activation and its effects on dendritic morphology. Nature Neurosci 4:151–158.

Yassa MA, Stark SM, Bakker A, Albert MS, Gallagher M, Stark CE. (2010) High resolution structural and functional MRI of hippocampal CA3 and dentate gyrus in patients with amnestic mild cognitive impairment. NeuroImage 51:1242–1252.

Yassa MA and Stark CE (2011) Pattern separation in the hippocampus. Trends Neurosci 34:515–525.

Yuste R and Bonhoeffer T (2004) Genesis of dendritic spines: insights form ultrastructural and imaging studies. Nature Rev Neurosci 5:24–34.

Yuste R (2011) Dendritic spines and distributed circuits. Neuron 71:772–780.

Zuo Y, Lin A, Chang P, Gan WB (2005) Development of long-term dendritic spine stability in diverse regions of cerebral cortex. Neuron 46:181–189.

LIBRARY RELEASE FORM

Publishing Agreement

It is the policy of the University to encourage the distribution of all theses, dissertations, and manuscripts. Copies of all UCSF theses, dissertations, and manuscripts will be routed to the library via the Graduate Division. The library will make all theses, dissertations, and manuscripts accessible to the public and will preserve these to the best of their abilities, in perpetuity.

Please sign the following statement:

I hereby grant permission to the Graduate Division of the University of California, San Francisco to release copies of my thesis, dissertation, or manuscript to the Campus Library to provide access and preservation, in whole or in part, in perpetuity.

Sachi Ifjim 9/18/2012

Author Signature Date